



Low dimensional physics using soft nanomaterials

Milan K. Sanyal
Surface Physics Division
Saha Institute of Nuclear Physics
1/AF, Bidhannagar, Kolkata-700 064

milank.sanyal@saha.ac.in

DAE-CEA Meeting, Sacly, France October 6-10, 2008



Center for Nanoscience and Surface Physics

(CENSUP)

Investigators:

Prof. M.K. Sanyal, Prof. D. Ghose, Prof. P. Chakraborty
Prof. A. Datta, Prof. S. R. Bhattacharyya, Prof. T. K. Chini
Prof. S. Kundu, Prof. M. Mukherjee, Prof. S. Hazra
Dr. Krishnakumar S. R. Menon, Dr. S. Bhunia

(Surface Physics Division, Saha Institute of Nuclear Physics)

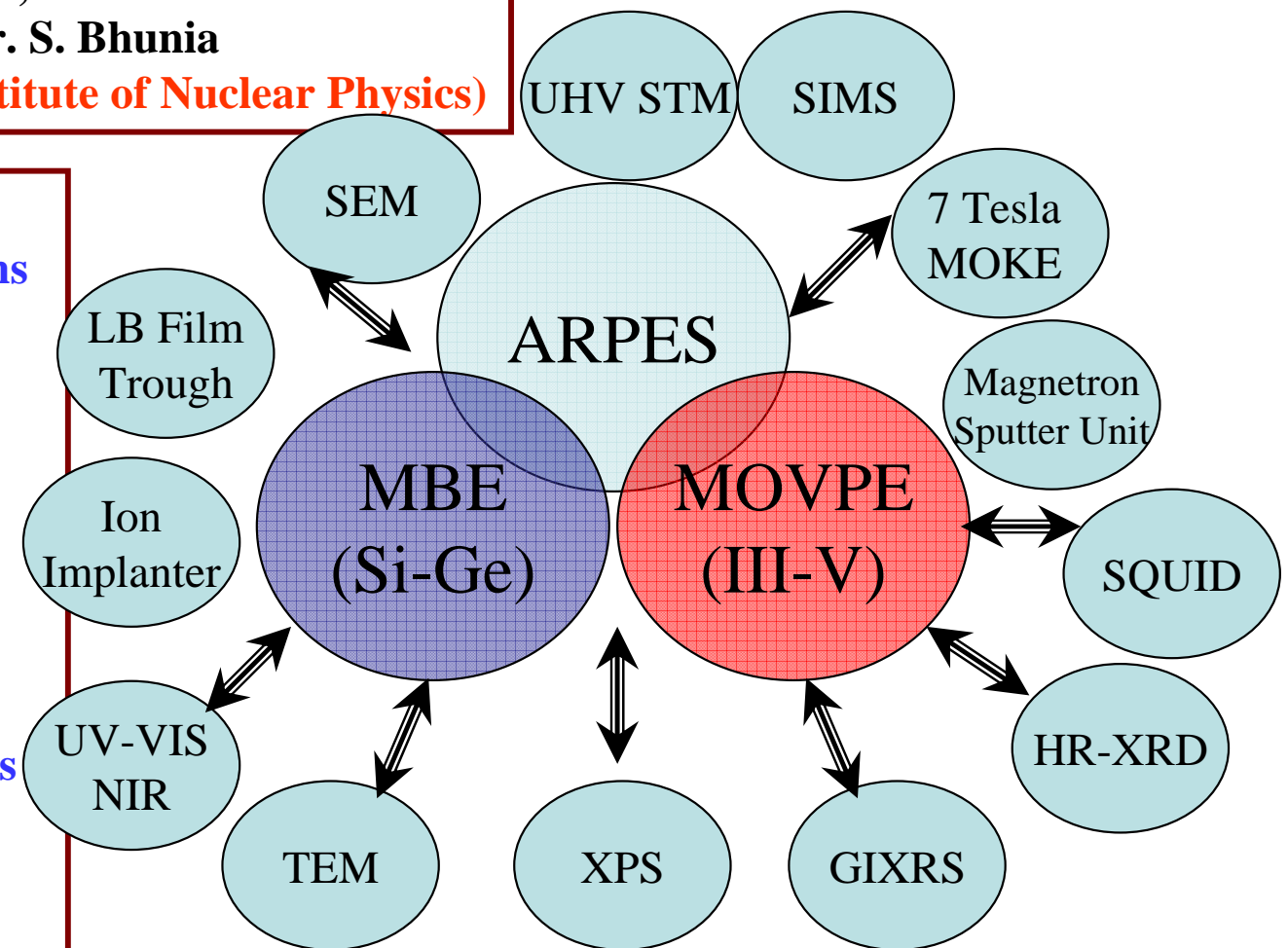
National and International participation in scientific programs

Development of inter-disciplinary research programs

Short term and long term exchange programs and schools

Development of world-class laboratory access to other facilities

To reduce time-gap between basic research and applications





18 15:04

Preparation Sample
Manipulator

Gamma-data UV lamp with
integrated Monochromator

LEED

Sample
Manipulator

Sample Load-Lock



Preparation Chamber
(Growth Chamber)

Analysis Chamber

Scienta R4000
Analyser

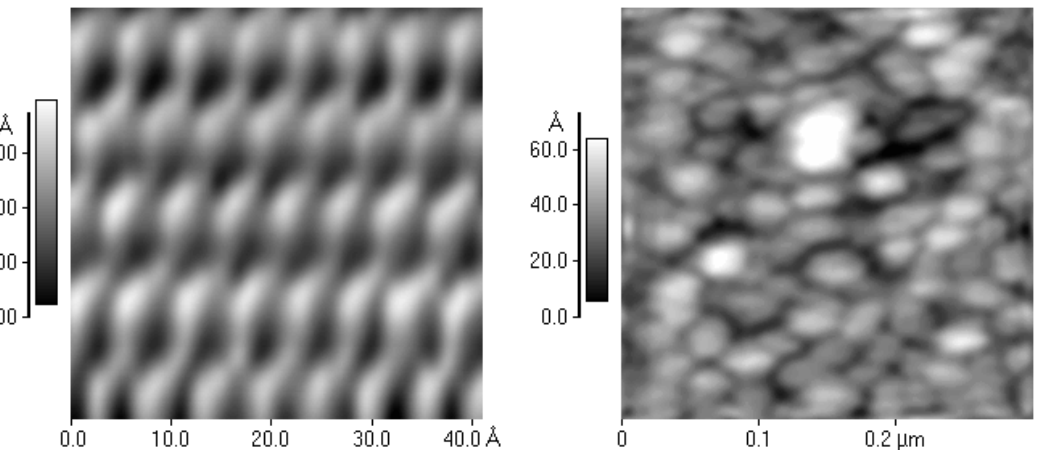
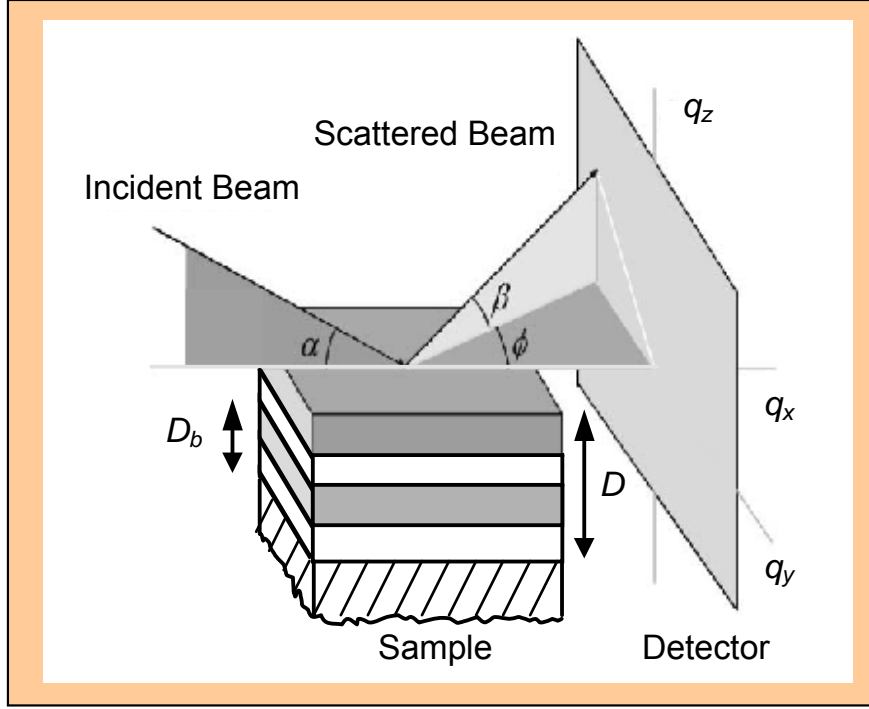
Plan of the talk:

- Nanomaterials  Low-dimensional Physics
- Structure, Magnetic ordering and electronic transport
- Verify and improve theoretical understanding
- Formation and ordering of nanoparticles at liquid-interfaces
- Formation of 1D Wigner Solids in polymer nanowires
- 2D magnetic ordering in Langmuir-Blodgett films



Thesis work of :

Atikur Rahman, Indranil Sarkar, Mrinal Bera and Sirshendu Gayen

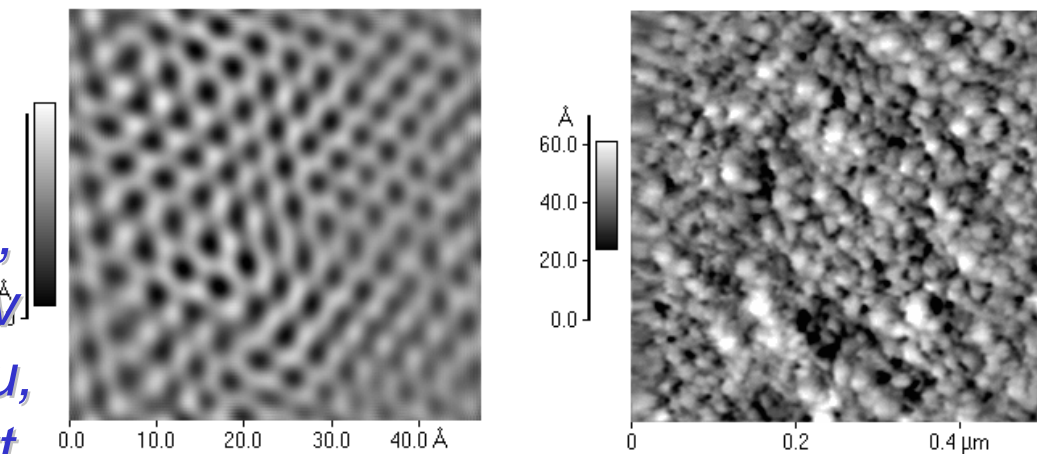


Out-of-plane structure

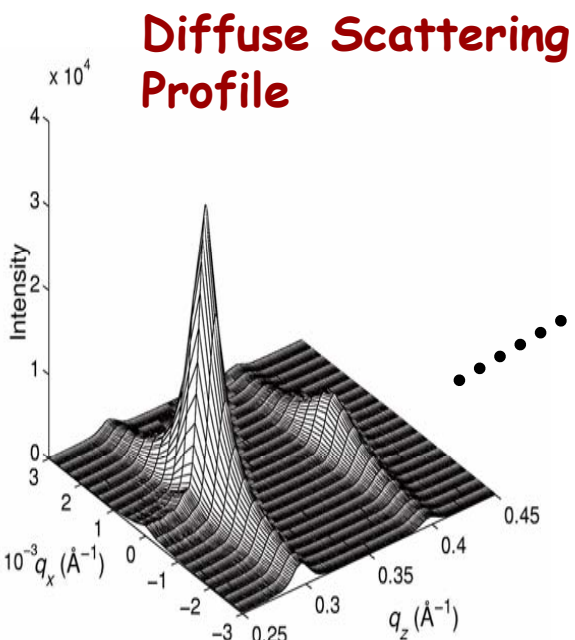
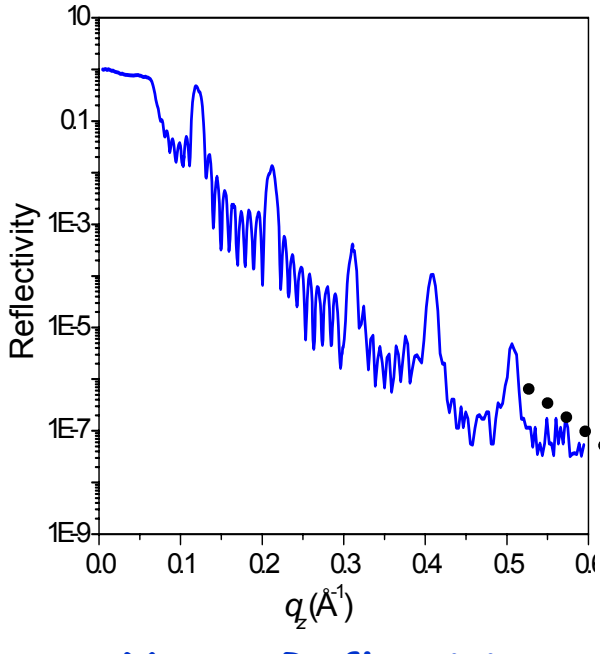
Sanyal, Mukhopadhyay, Mukherjee,
Datta, Basu and Penfold, Phys. Rev.
B65, 033049 (2001) & Sanyal, Basu,
Datta and Banerjee, Europhys. Lett.
36, 265 (1996)

In-plane structure

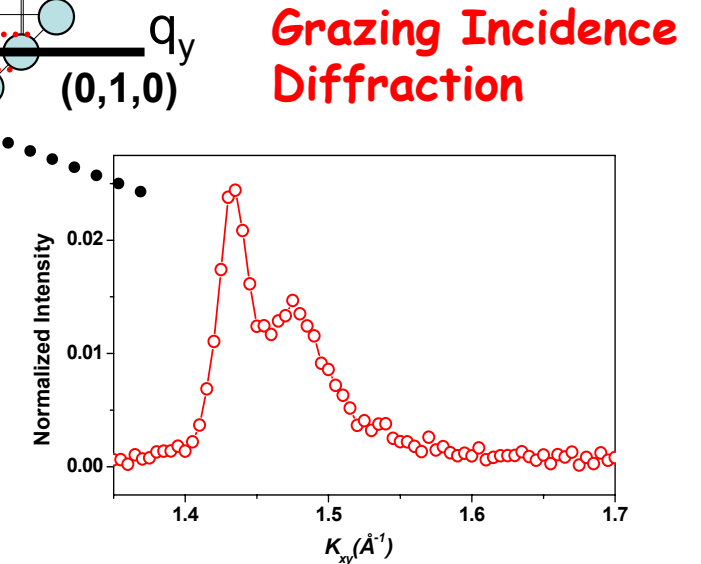
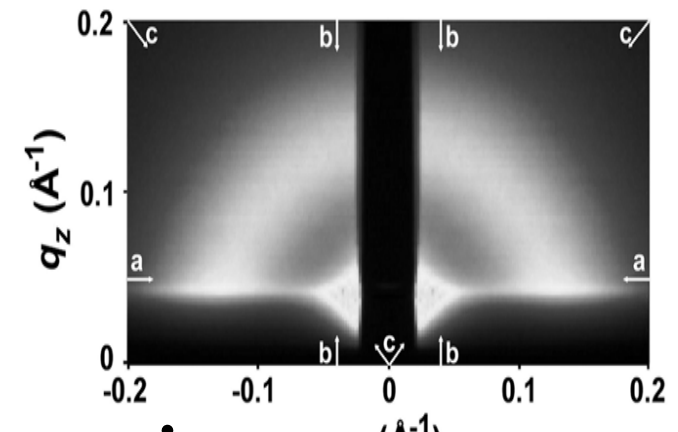
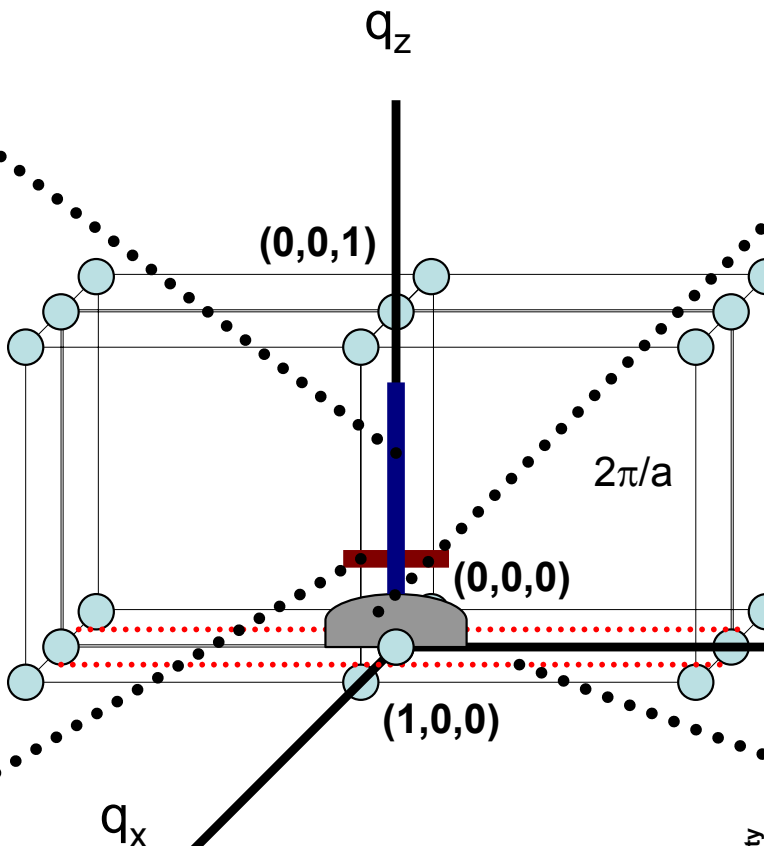
Basu, Hazra and Sanyal, Phys. Rev.
Lett. 82, 4675 (1999) & Basu and
Sanyal, Phys. Rev. Lett. 79, 4617
(1997).

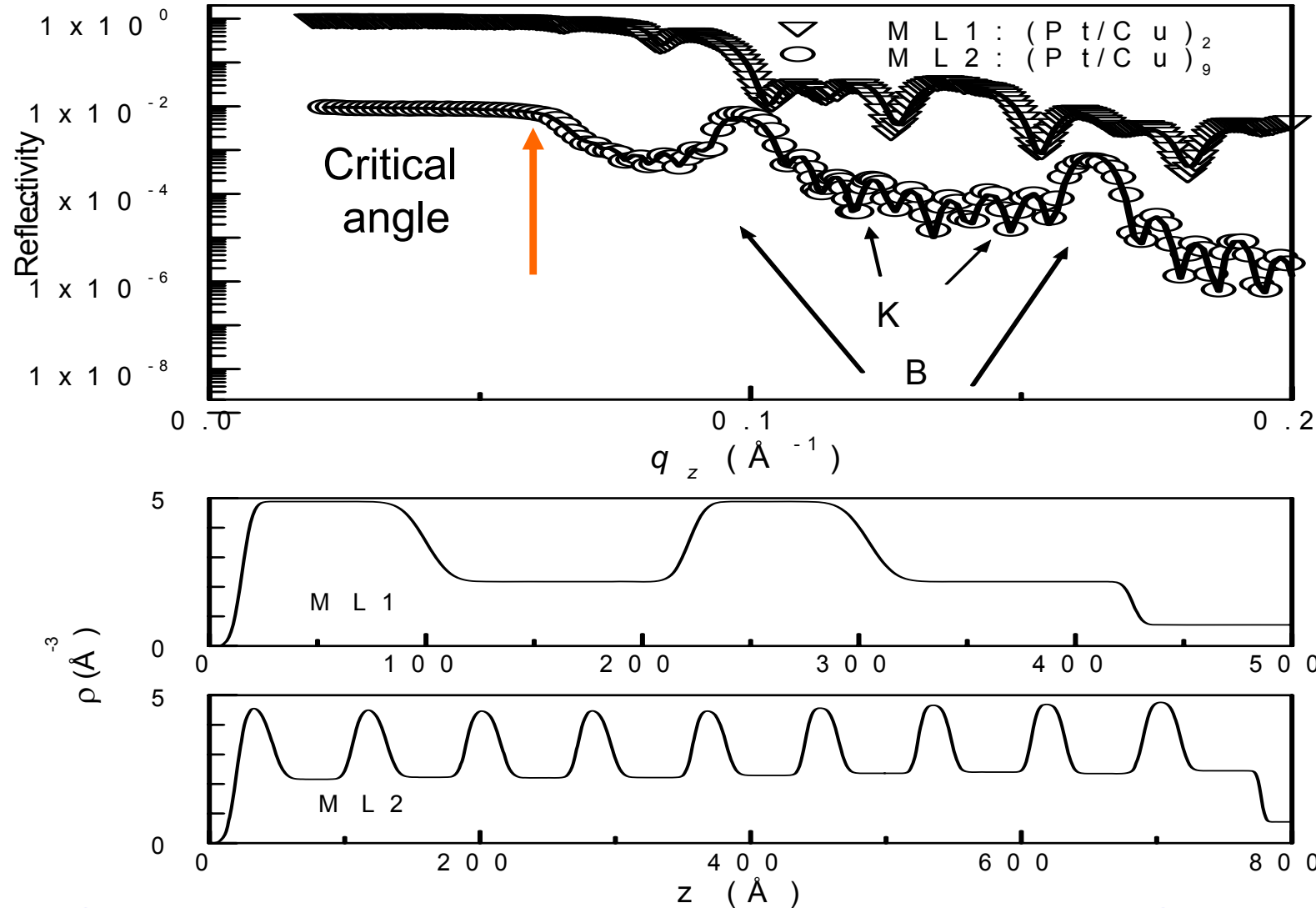


Information in real and
reciprocal space



X-ray Scattering To study structure And Morphology

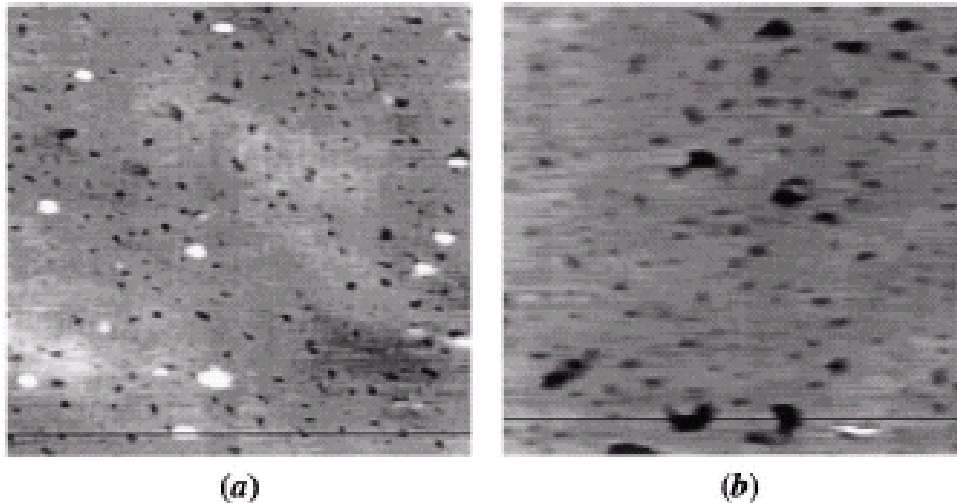




Reflectivity peaks and Keissig fringes Extraction of EDP is nontrivial

Sanyal, Basu, Datta and Banerjee, [Europhys. Lett. 36](#), 265 (1996)

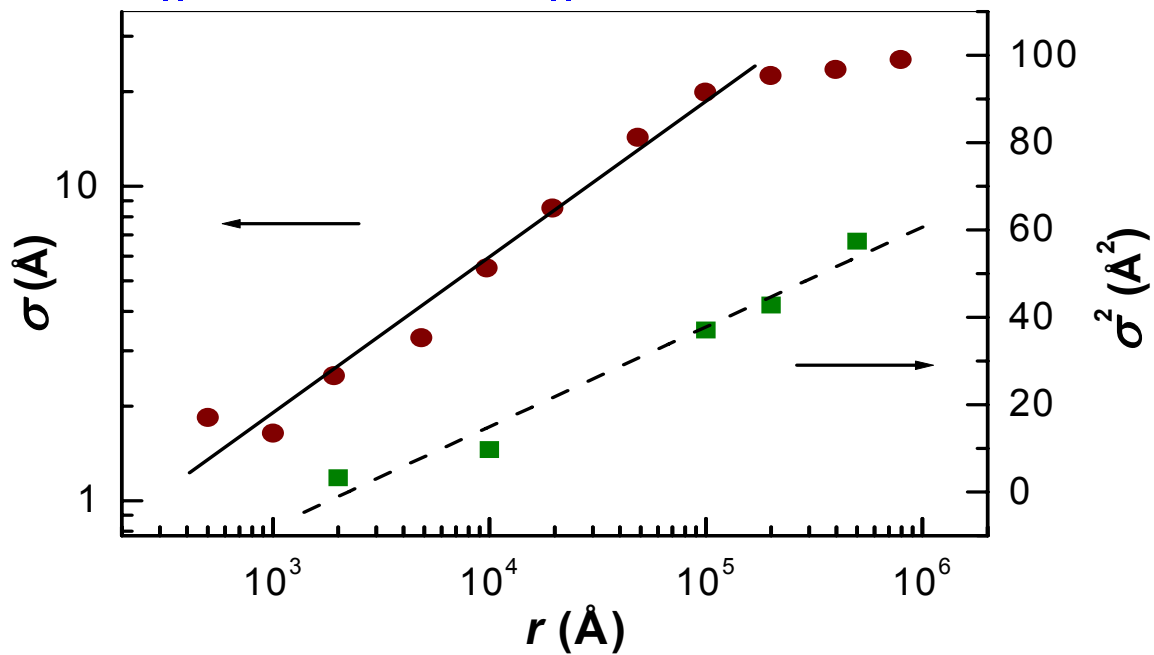
Sanyal, Hazra, Basu and Datta, [Phys. Rev. B 58](#), R4258 (1998).



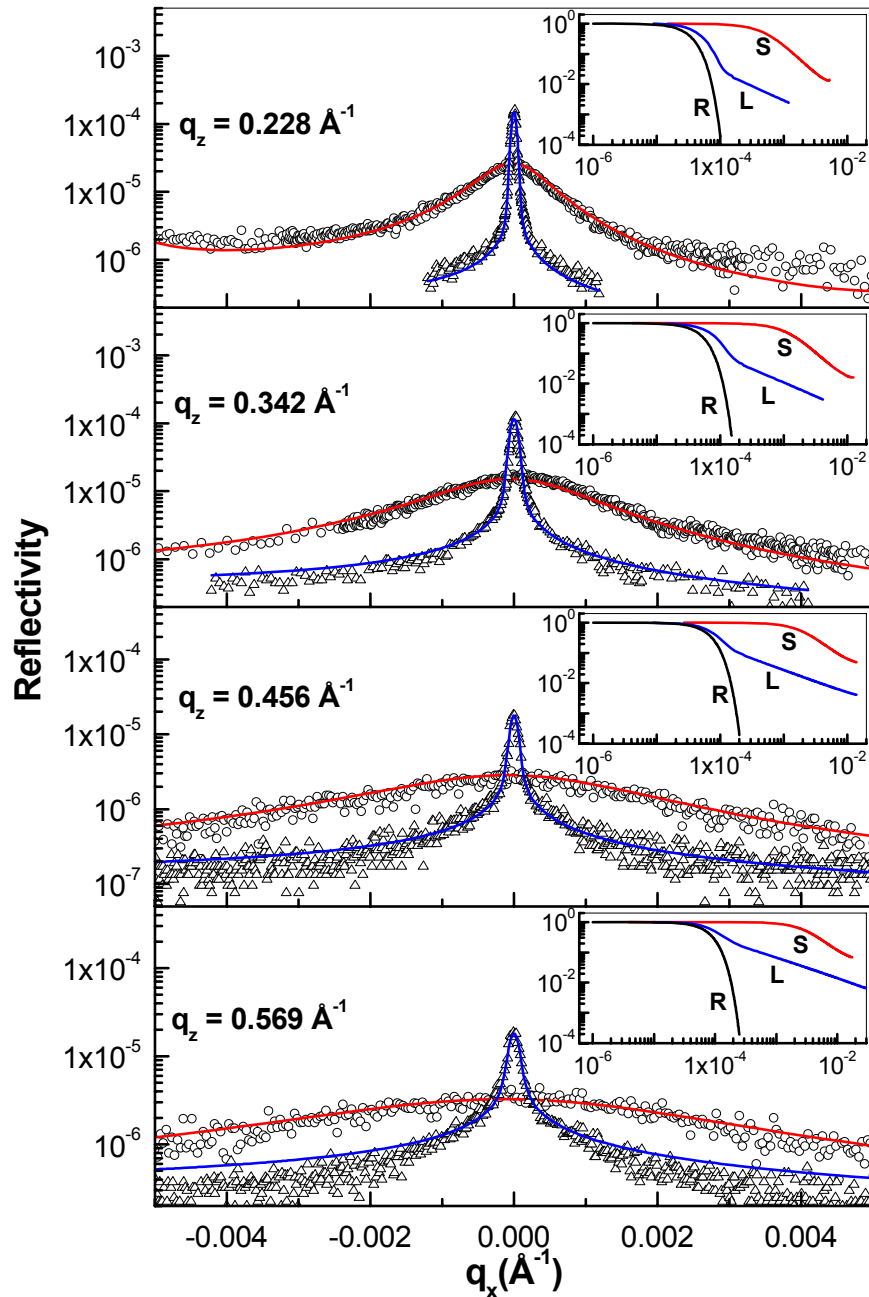
Height difference correlation function

$$g(r_{\parallel}) \equiv \langle [z(0)-z(r_{\parallel})]^2 \rangle = 2\sigma^2 - 2C(r_{\parallel})$$

With $C(r_{\parallel}) \equiv \langle z(0)z(r_{\parallel}) \rangle$ & roughness σ



Growth mechanism of Langmuir-Blodgett film



1D transfer (diffusion) in the water-substrate Contact line

2D adsorption on the substrate after transfer of molecules - symmetric molecular orientation.

Out-of-plane structure

Sanyal, Mukhopadhyay, Mukherjee, Datta, Basu and Penfold, Phys. Rev B65, 033049 (2001).

In-plane structure

Basu, Hazra and Sanyal, Phys. Rev. Lett. 82, 4675 (1999) & Basu and Sanyal, Phys. Rev. Lett. 79, 4617 (1997).

Scattering from capillary wave correlation

$$\frac{d\sigma}{d\Omega} = \frac{\rho_{el} r_e^2 A}{q_z^2} (e_{in} \cdot e_{sc}) \int dr e^{iq \cdot r} \exp(-\frac{1}{2} q_z^2 g(r))$$

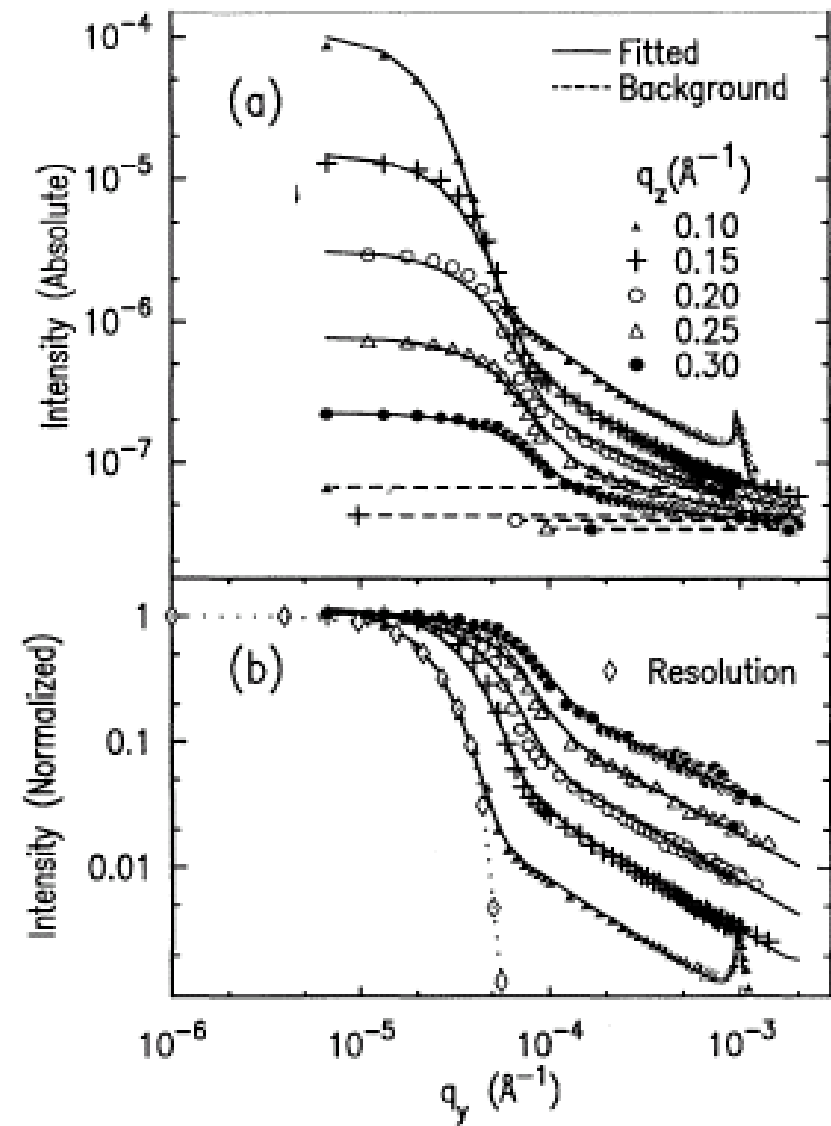
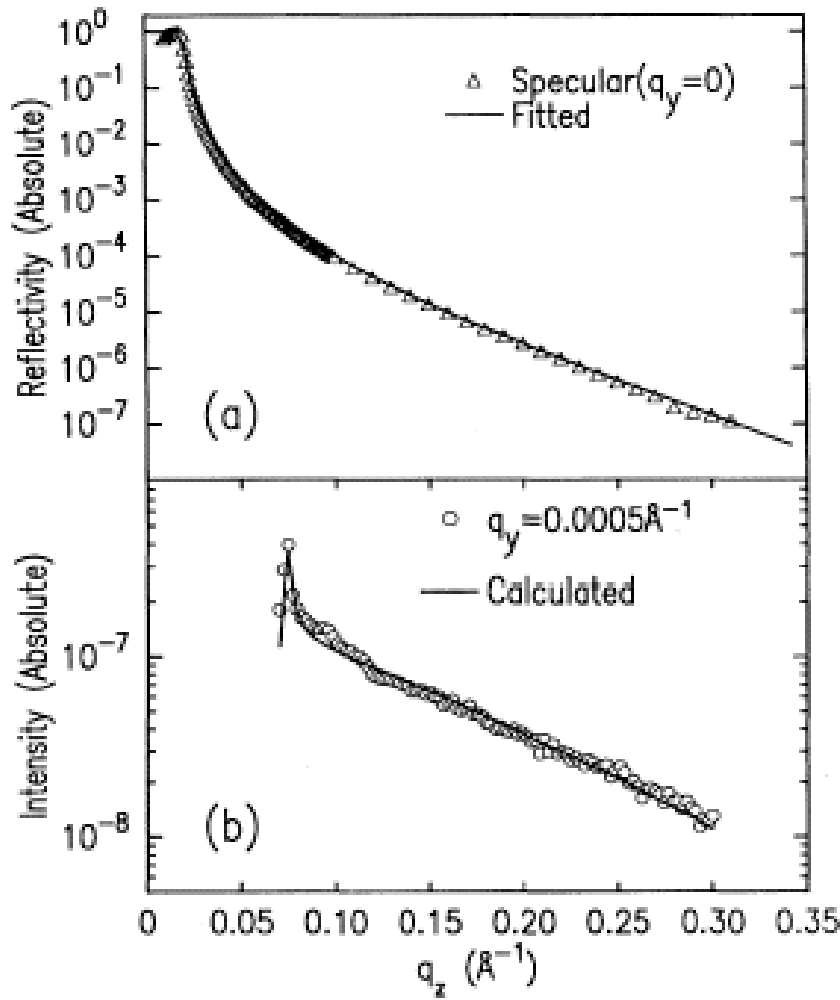
$$I = I_0 \frac{q_c^4}{16} \frac{1}{q_z^3} \frac{1}{2k_0 \sin \alpha} \exp(-q_z^2 \sigma^2) \frac{1}{\sqrt{\pi}} \Gamma(\frac{1-\eta}{2}) F(q_x)$$

$$F(q_x) = {}_1F_1\left[\frac{1-\eta}{2}; \frac{1}{2}; \frac{q_x^2 L^2}{4\pi^2}\right] |T(\alpha)|^2 |T(\beta)|^2$$

Hypergeometric Kummar function

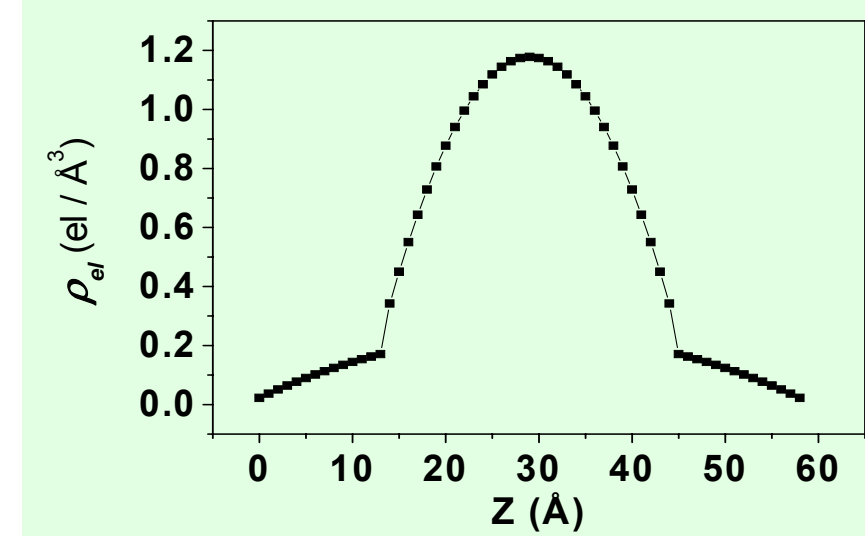
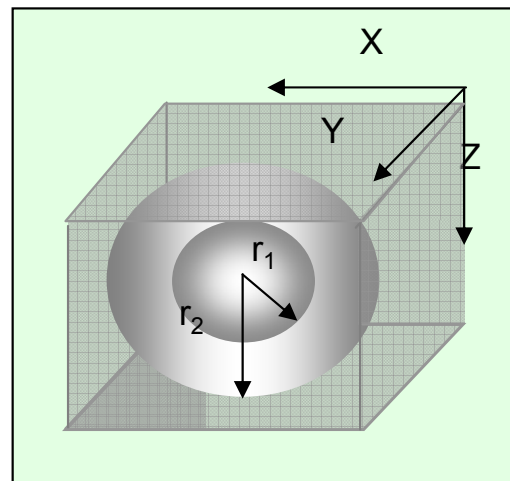
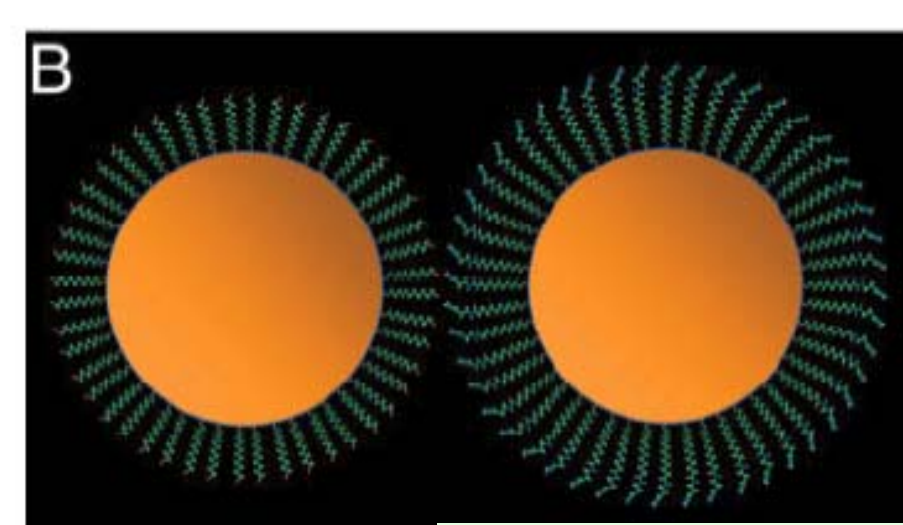
Sanyal, Sinha, Huang and Ocko, Phys. Rev. Lett. 66, 628 (1991)

$$R = R_F \exp(-q_z^2 \sigma_{eff}^2) \frac{1}{\sqrt{\pi}} \Gamma(\frac{1-\eta}{2})$$



Verification with ethanol surface

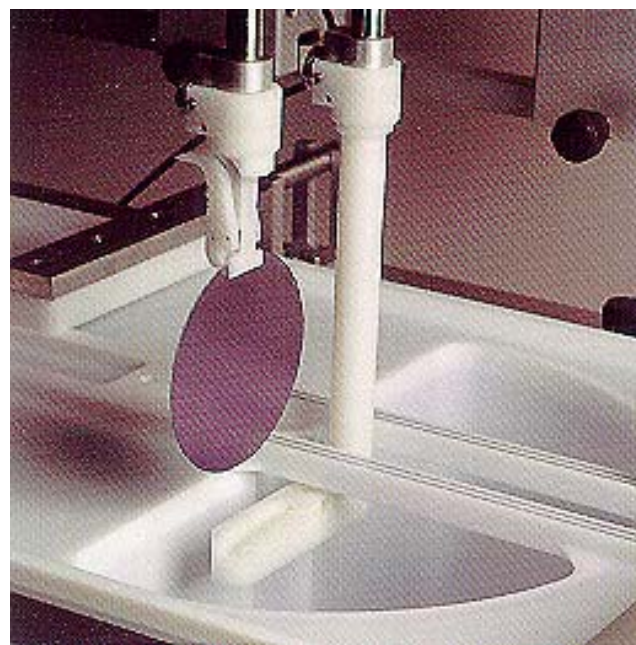
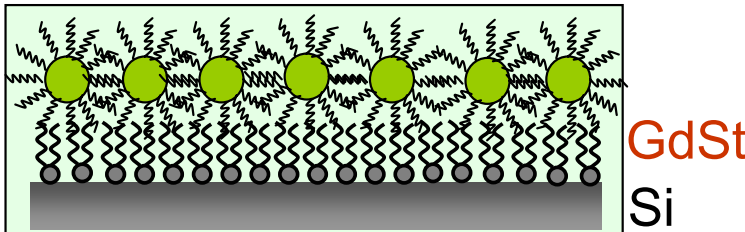
Thiol-capped GOLD nano-particles



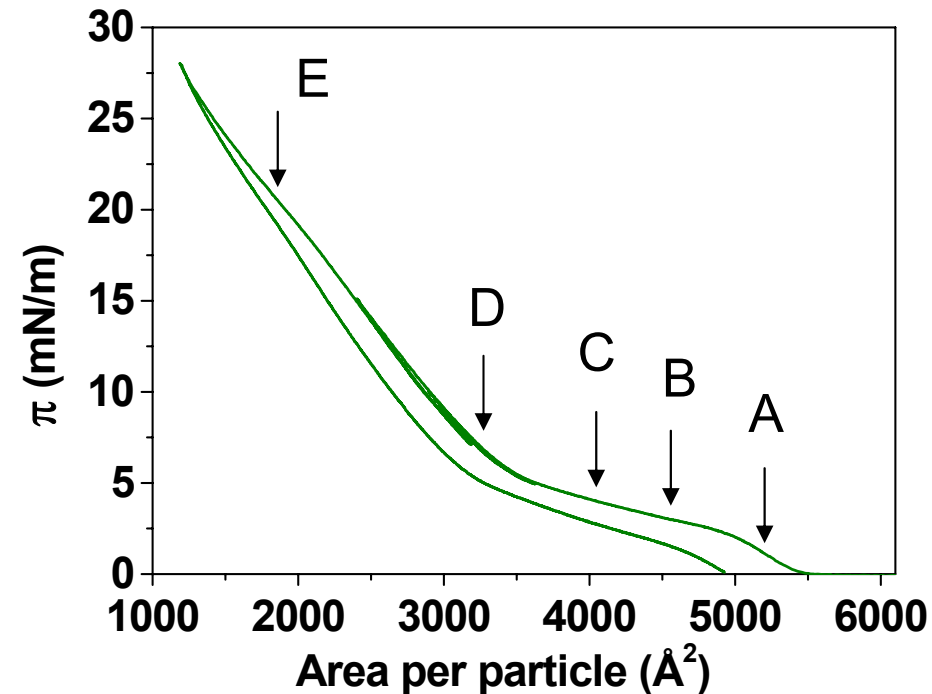
J. R. Heath, C. M. Knobler, and D. V. Leff, J. Phys. Chem. B 101, 189 (1997);
M. Fukuto, R. K. Heilmann, P. S. Pershan, A. Badia, and R. B. Lennox,
J. Chem. Phys. 120, 3446 (2004); M. Brust et. al. Chem. Commun. 1994, 801.

Growth of Au nanoparticle film on GdSt/Si(001) by Langmuir-Blodgett technique

Au nanoparticle film

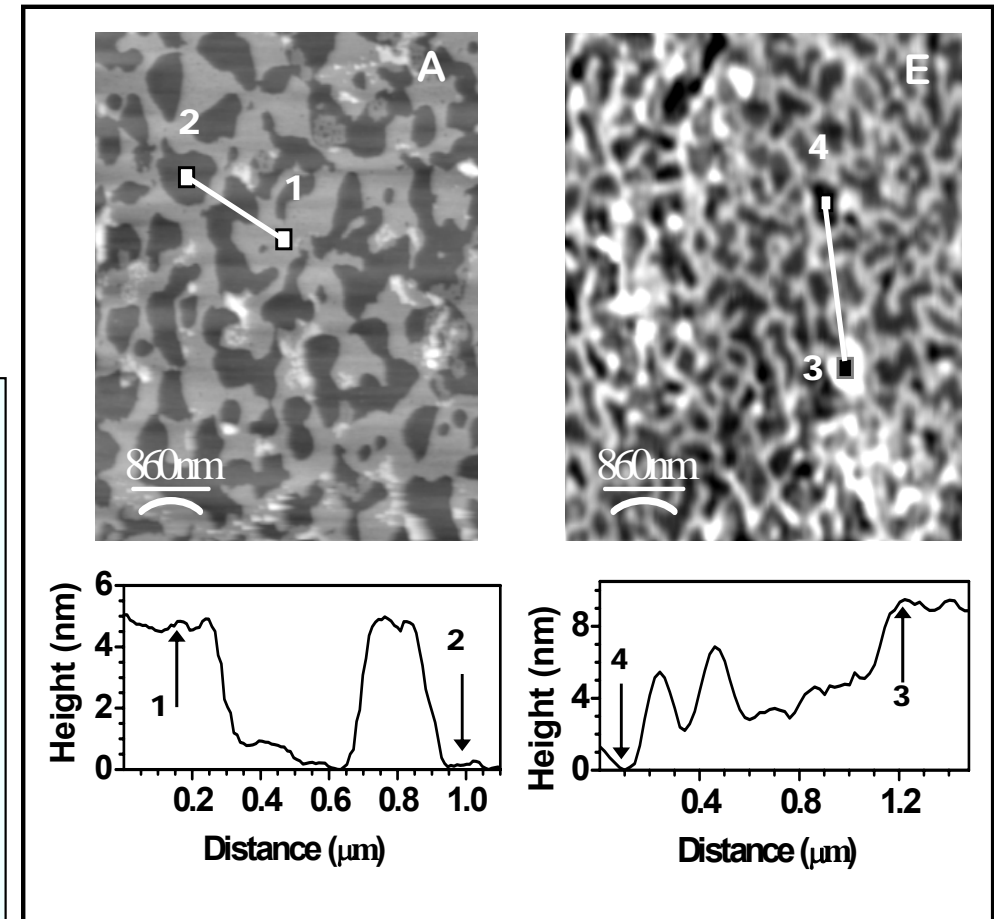
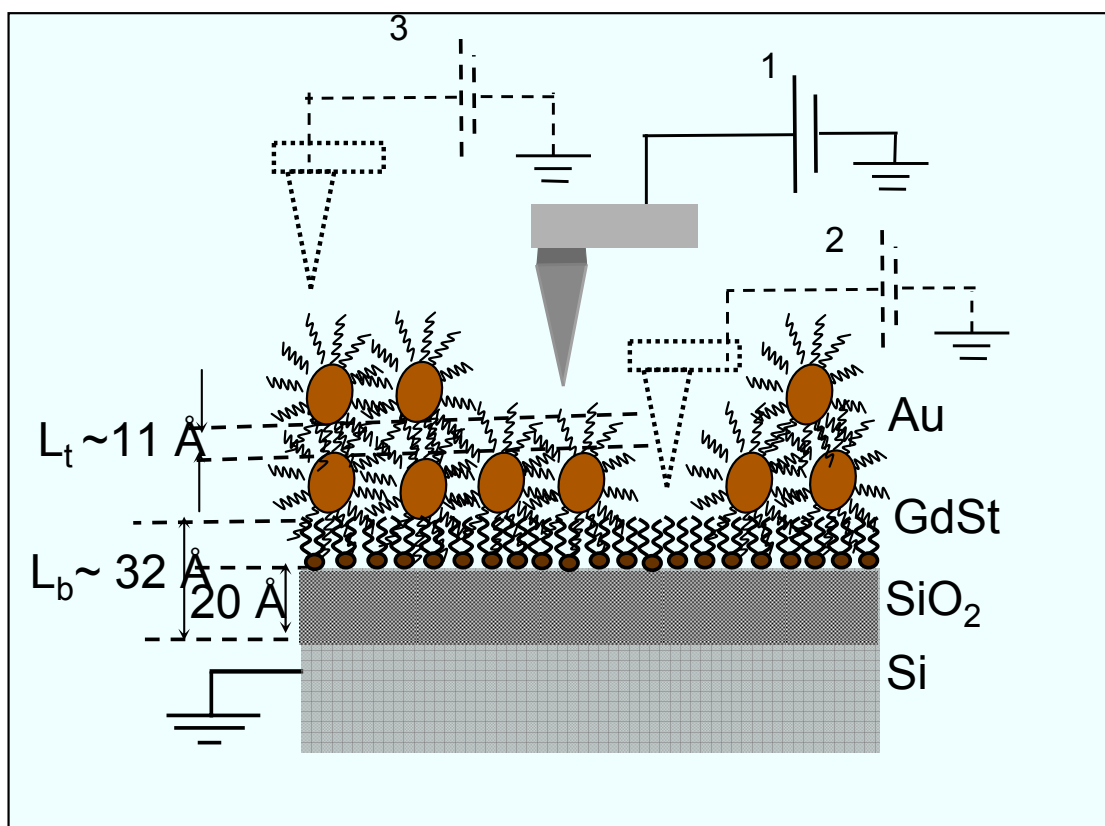
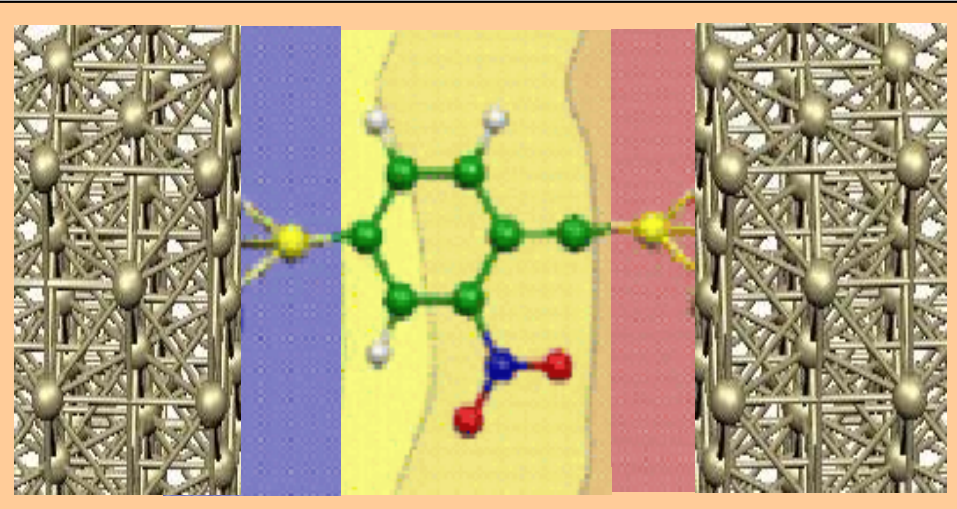


Dodecanethiol encapsulated Au nanoparticles (**average diameter 33Å**) prepared by Brust method

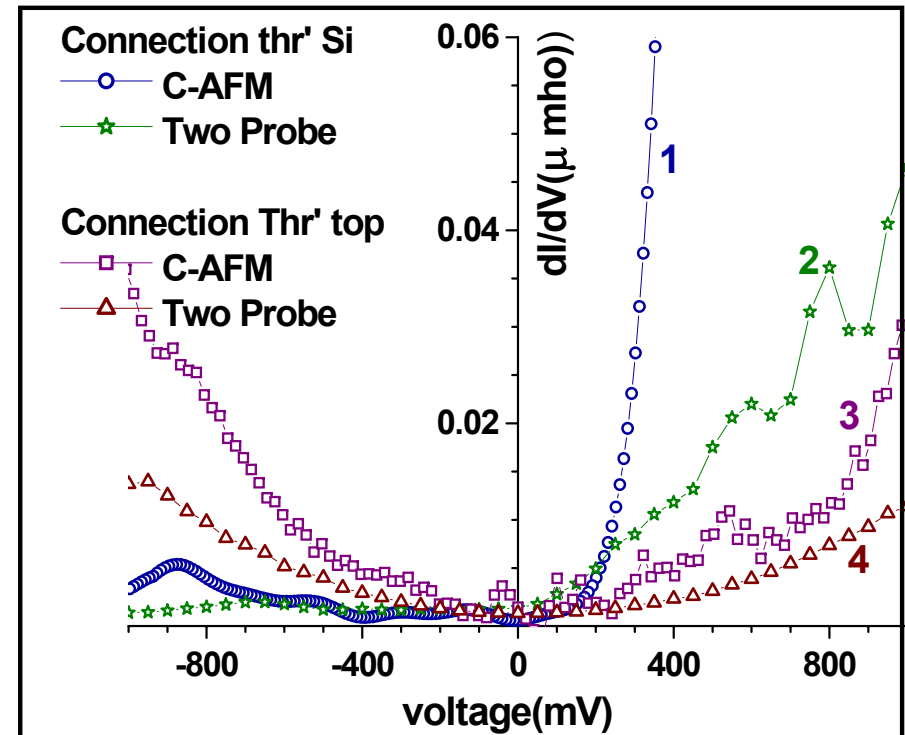
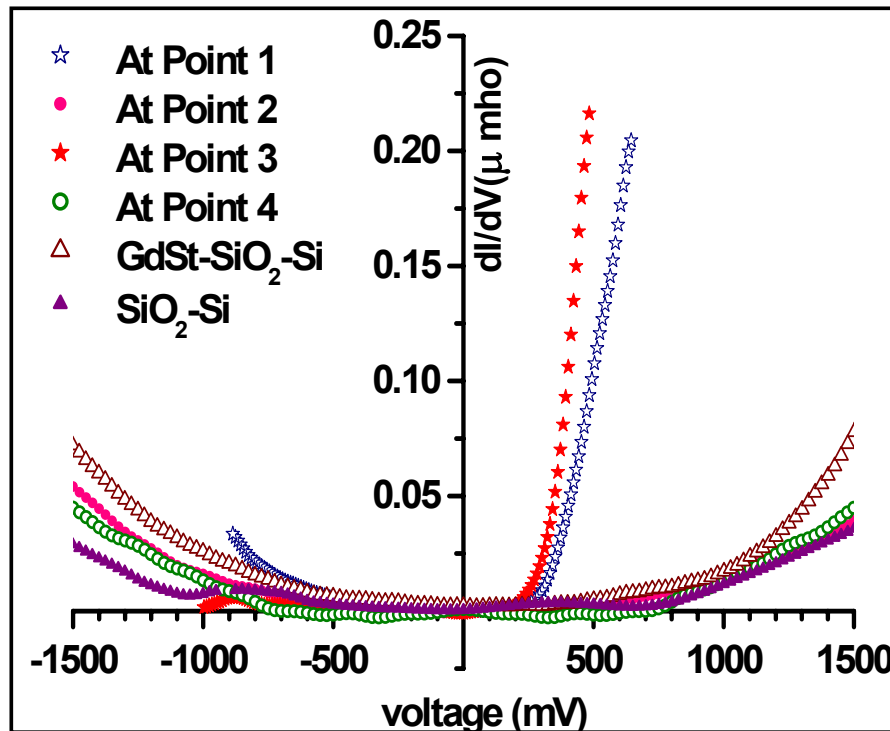


Five films A, B, C, D and E deposited at monolayer pressure of 1.5, 2.5, 3.5, 7.0 and 20.0 mN/m respectively

Study of transport properties through single nanoparticle

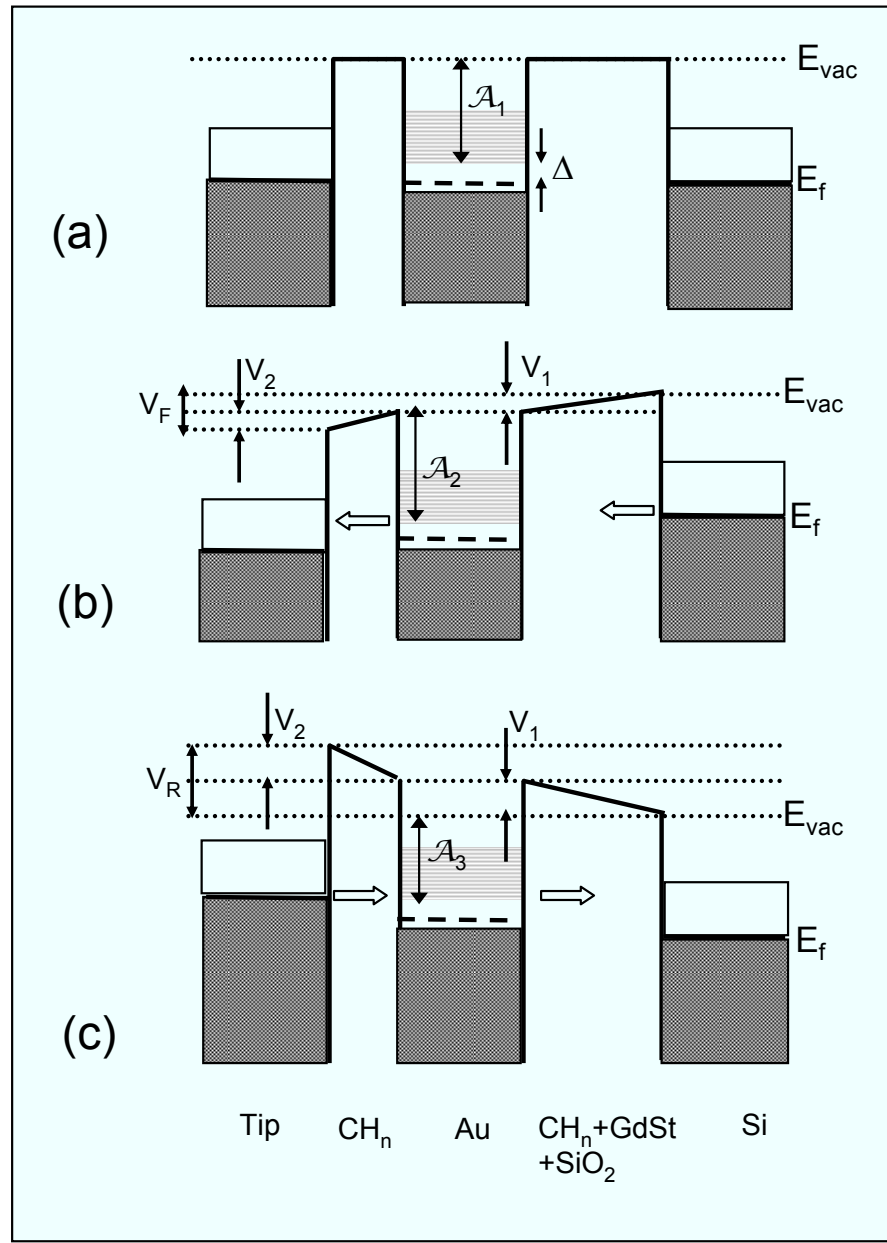


I-V Characteristics:



Rectification ratio $R \sim$ ratio of forward to reverse current at ± 500 mV :
13.5 for monolayer film & **364.8** for bilayer film

S. Pal, M. K. Sanyal, N. S. John and G. U. Kulkarni,
 Phys. Rev. B 71, 121404(R), 2005



Voltage drop at bottom and top barrier:
 V_b and V_t respectively

$$\text{Assymmetric factor, } \eta = V_b / V_t$$

Energy gap in Au nanocluster
 $\Delta = (E_{vac} - E_f) - \mathcal{A}_1$

Forward voltage $V_F \rightarrow$ Silicon Fermi level lines up with conduction level of Au nanocluster $eV_F = \Delta(1+\eta)/\eta$

Corresponding reverse voltage
 $eV_R = \Delta(1+\eta)$

$$\eta = V_R / V_F = 1.9 \quad \Delta \sim 155 \text{ meV}$$

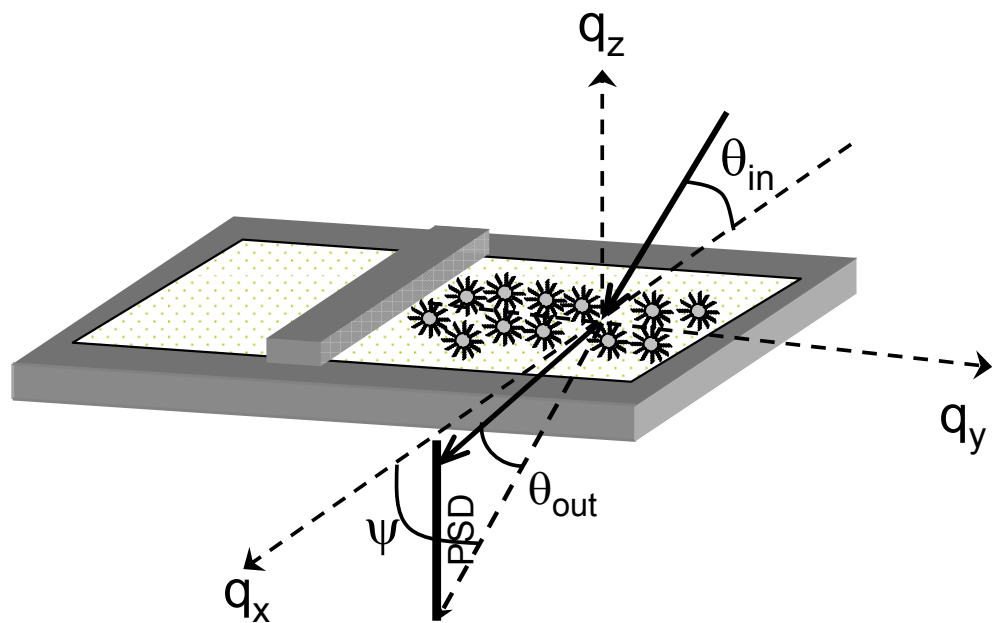
W. Tian, S. Datta, S. Hong, R. Reifenberger, J. I. Henderson and C. P. Kubiak, J. Chem. Phys. 109, 2874, (1998); P. E. Kornilovitch, A. M. Bratkovsky and R. S. Williams, Phys. Rev. B 66, 165436, (2002).

Monolayer of thiol-capped gold nanoparticles at air-water interface: reversible buckling

In-plane structure of 2D Langmuir monolayer of Au nanoparticles on water surface



Plays key role in determining surface morphology of deposited Au/GdSt/Si film



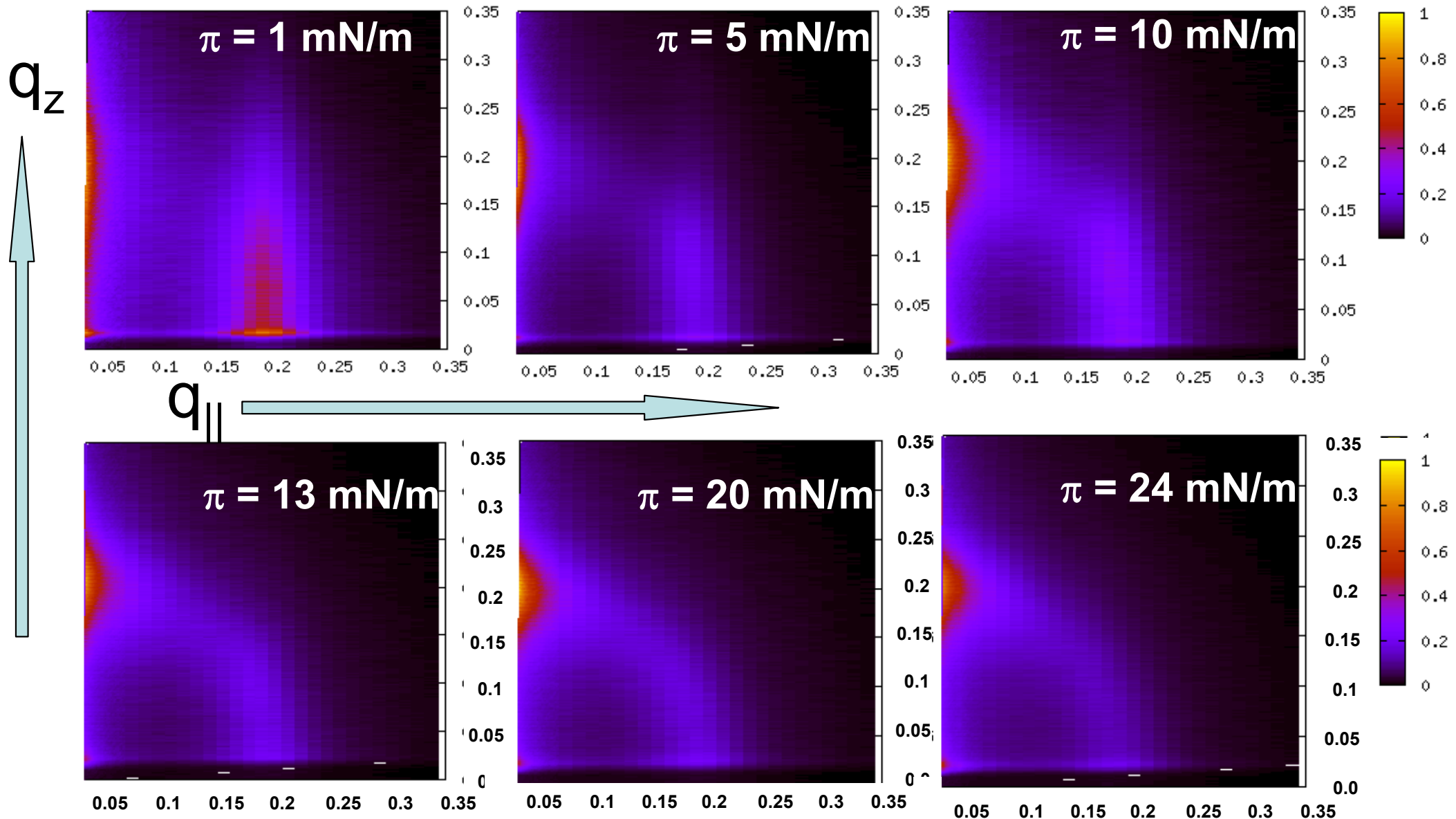
Dodecanethiol encapsulated Au nanoparticles prepared by Brust method

GID & diffuse scattering study at ID10B beamline of ESRF with nanoparticles of 20 Å diameter

M. K. Bera, M. K. Sanyal, S. Pal, J. Daillant, A. Datta, G. U. Kulkarni, D. Luzet and O. Konovalov, *Europhysics Lett.* 78, 56003 (2007).

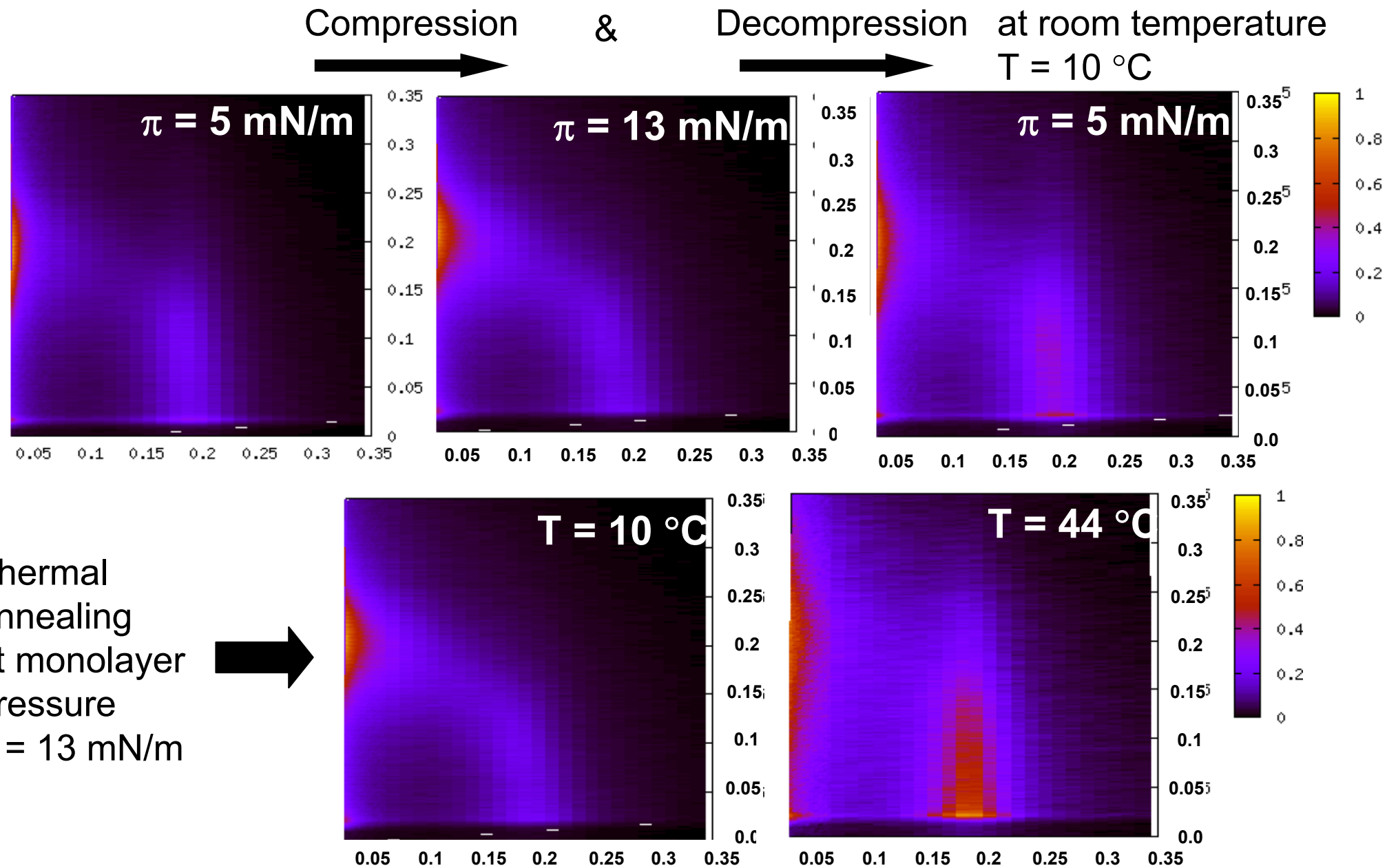
Experimental Results

X-ray scattering measurements done at room temperature $T = 10 \text{ } ^\circ\text{C}$.



Transformation of **Bragg Rod** to **Arc** with the increase in surface pressure

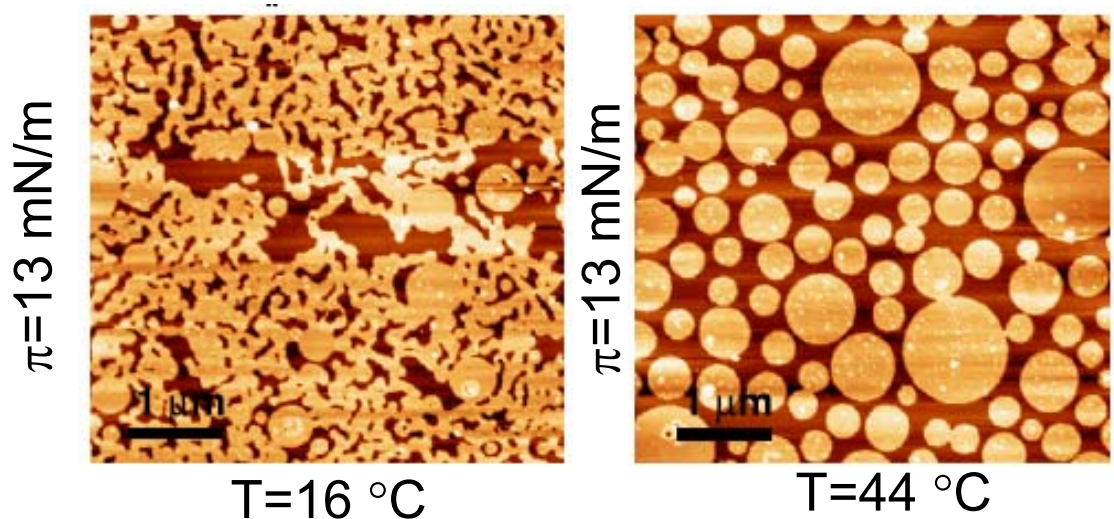
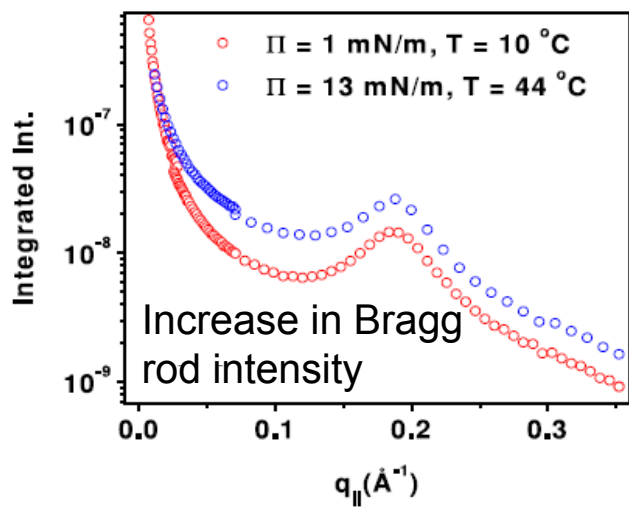
Experimental Results Continued...



Bragg rod can be straightened by decompression or Thermal annealing

Conclusion

- The formation of 2D monolayer takes place in the form of islands even at very low surface pressure due to self-organization, which is evident from Bragg rod at low pressures.
- With the increase in surface pressure first the islands come closer to each other along the direction of compression and starts random buckling before the formation of bilayer.
- The monolayer can be regained from buckled phase either by decompression or by thermal annealing. Thermal annealing at higher surface pressure actually increases the surface coverage which can be a possible route to increase the surface coverage beyond 60 %.



The Motivation



Nanocrystalline film of Au formed at the toluene–water interface.

- triphenylphosphine gold chloride +
tetrakishydroxymethylphosphonium chloride (THPC)

C. N. R. Rao et al, *J. Colloid Interface Sci.* 289, 305 (2005).

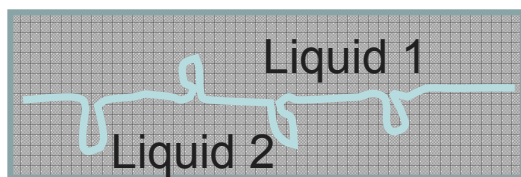
Formation and Ordering in Cofinement

- **Chemical Reactions at liquid-liquid interface**

Liquid Chromatography,, Phase-transfer catalysis,
drug delivery, membrane biophysics

- **Chemical Reactions & Microscopic structure of interface**

Formation of finger like structures of ~1 nm at the interface



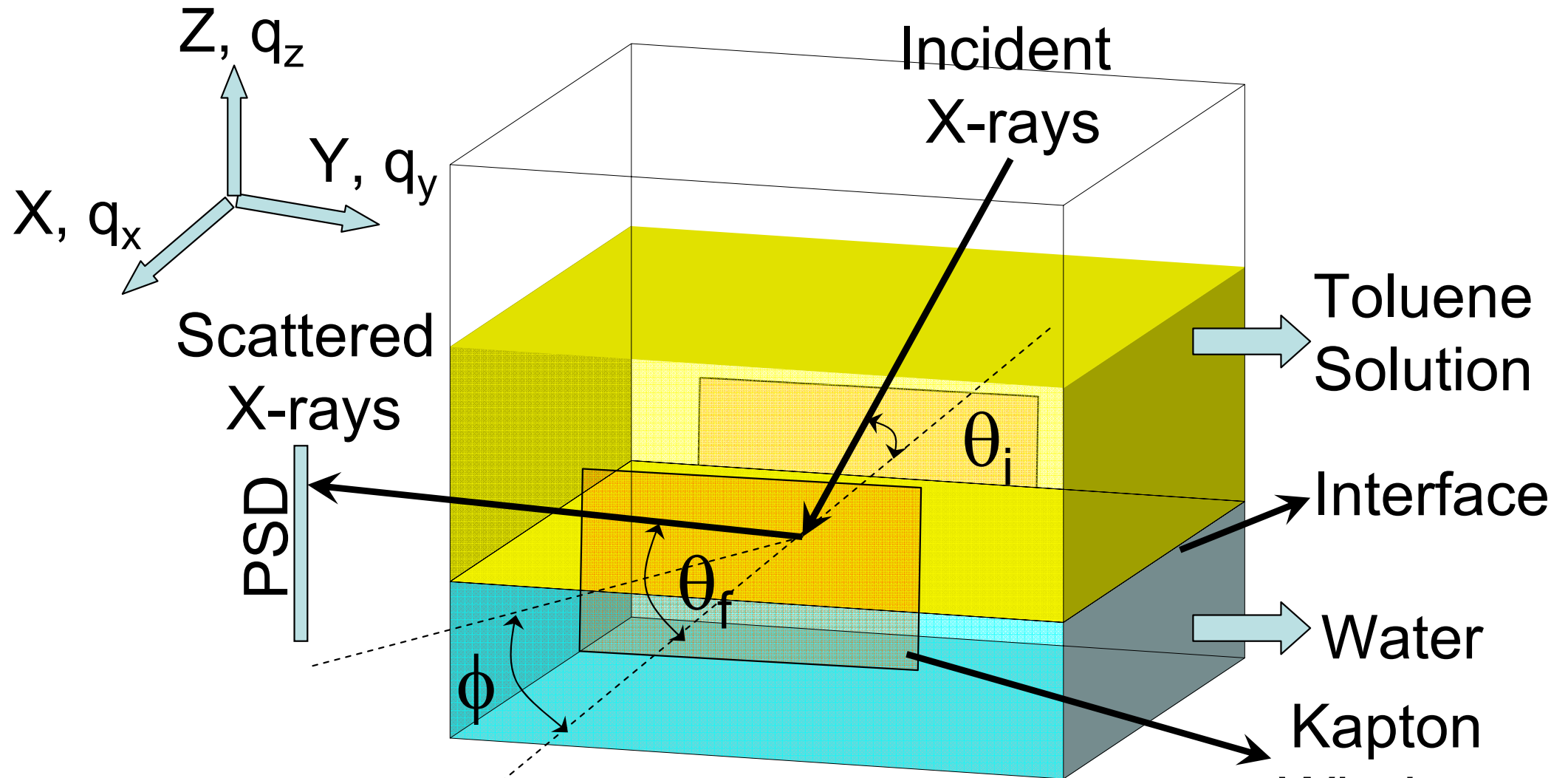
Chem. Rev. 1996, **96**, 14419-1476

- **Availability of High Energy Synchrotron x-rays**

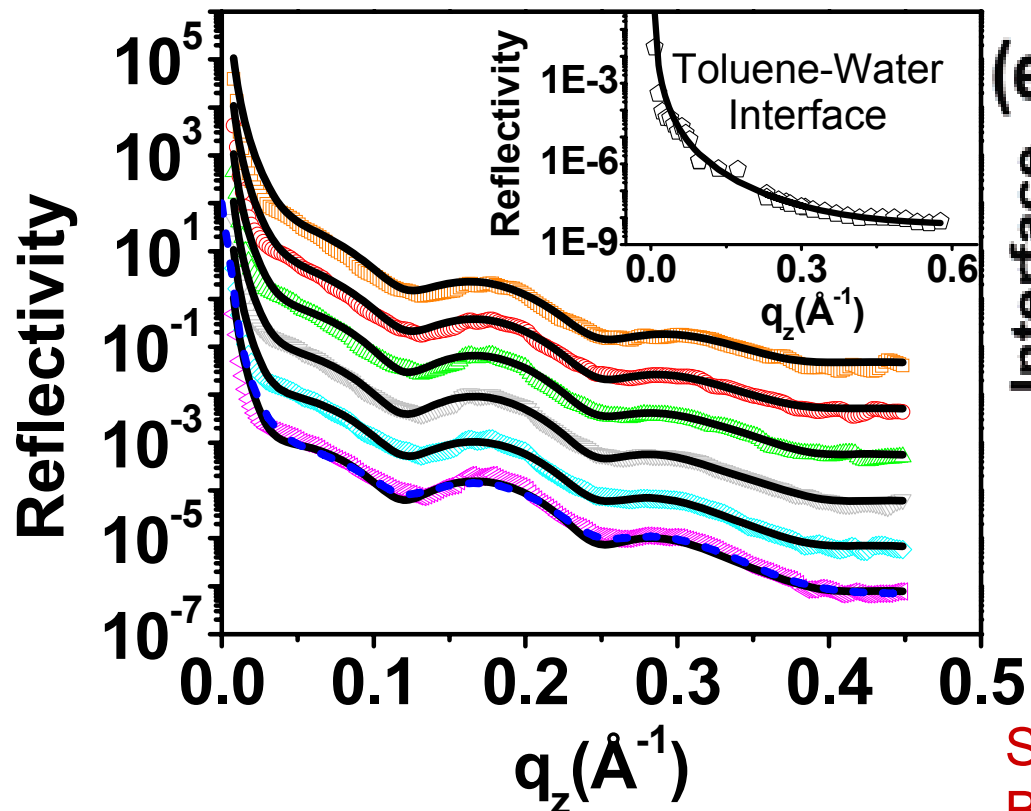
X-ray scattering techniques can probe interfacial structures as well as the materials formed at the interface

Phys. Rev. Lett. 1991, **66**, 628-631
Science, **311**, 216,218

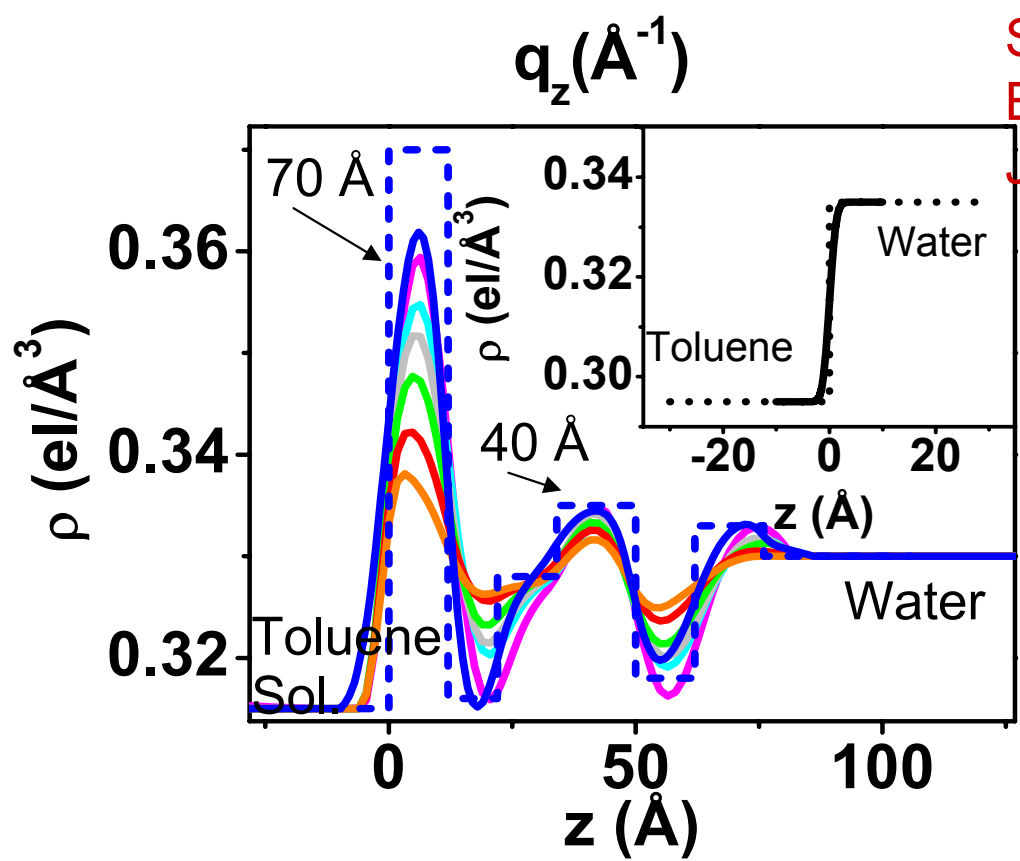
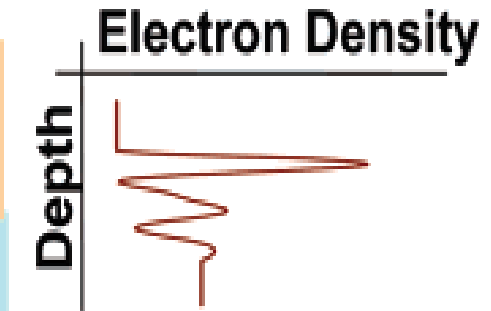
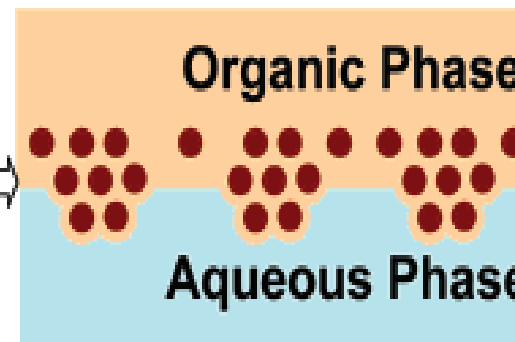
- Molecular ordering accompanying chemical reactions at liquid-liquid interface could not be understood through electron microscopy, optical spectroscopy and x-ray diffraction studies of transferred films.
- In-situ X-ray scattering study is important to understand chemical reactivity in inhomogeneous environment and ion/charge transfer processes across interfaces, which is sensitive to the presence of microscopic roughness, which is related to macroscopic interfacial tension through capillary wave theory.
- It is known that water "fingers" and organic "fingers" protrude into one another (as large as 0.8nm) to facilitate interfacial chemical reaction.



- (a) Fradin, C.; Luzet, D.; Braslau, A.; Alba, M.; Muller, F.; Daillant, J.; Petit J. M.; Rieutord, F *Langmuir* 1998, 14, 7327.
- (b) Mitrinovic, D. M.; Zhang, Z.; Williams, S. M.; Huang, Z.; Schlossman, M. L. *J. Phys. Chem. B* 1999, 103, 1779.
- (c) Martin, E. S.; Konovalov, O.; Daillant, J. *Thin Solid Films* 2007, 515, 5687.



(e)



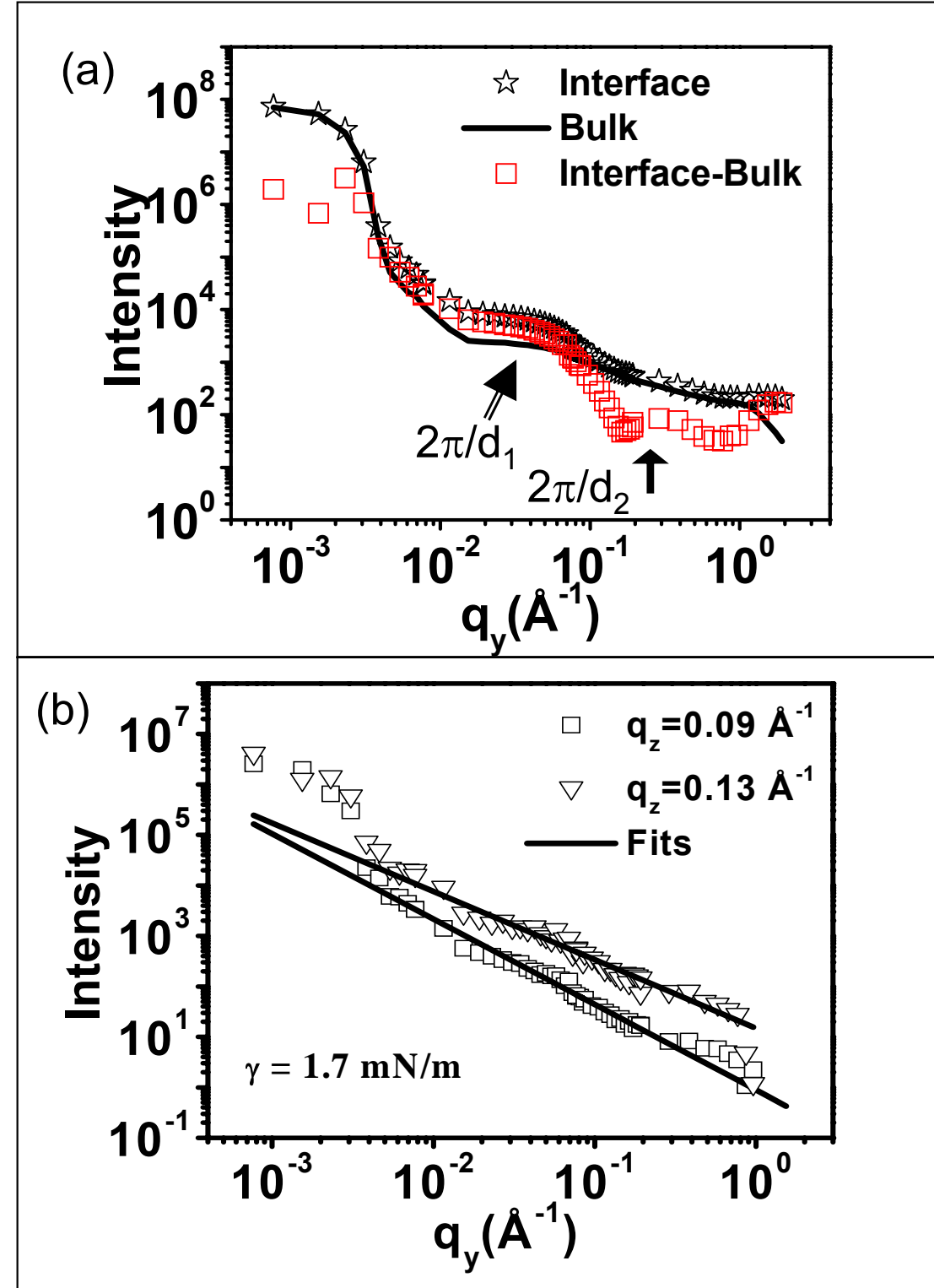
Sanyal, Agrawal, Bera, Kalyanikutty, Daillant, Blot, Kubowicz, Konovalov and Rao,
J. Phys. Chem. C 112, 1739 (2008)

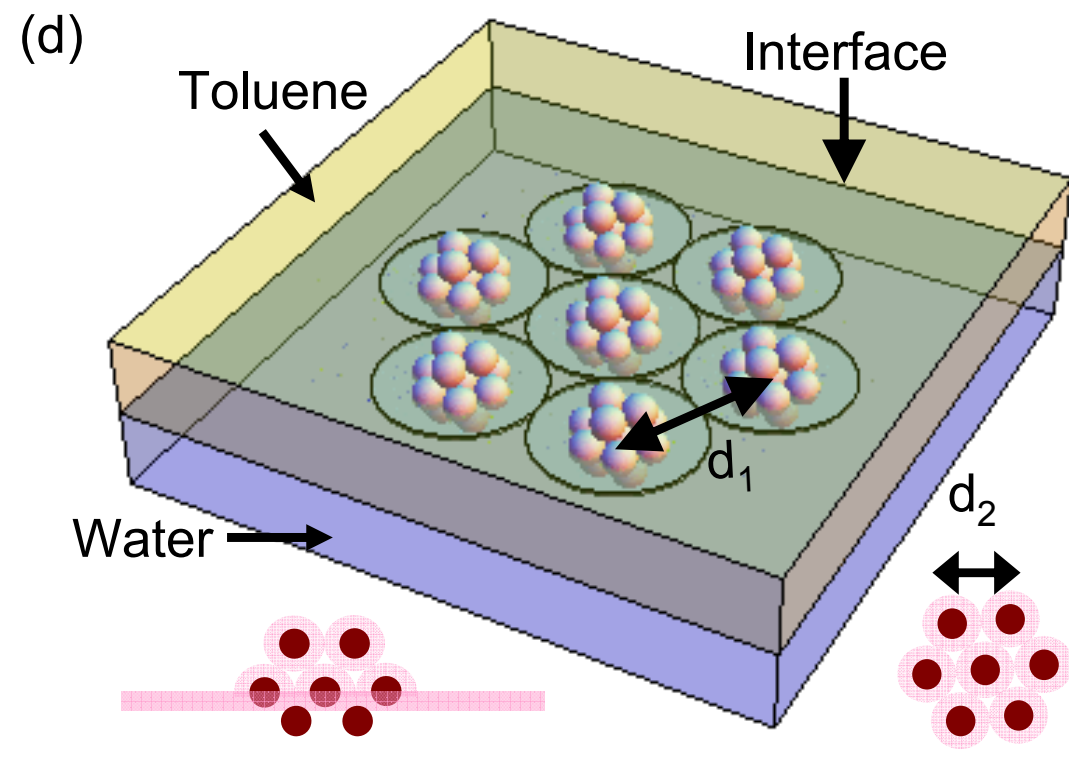
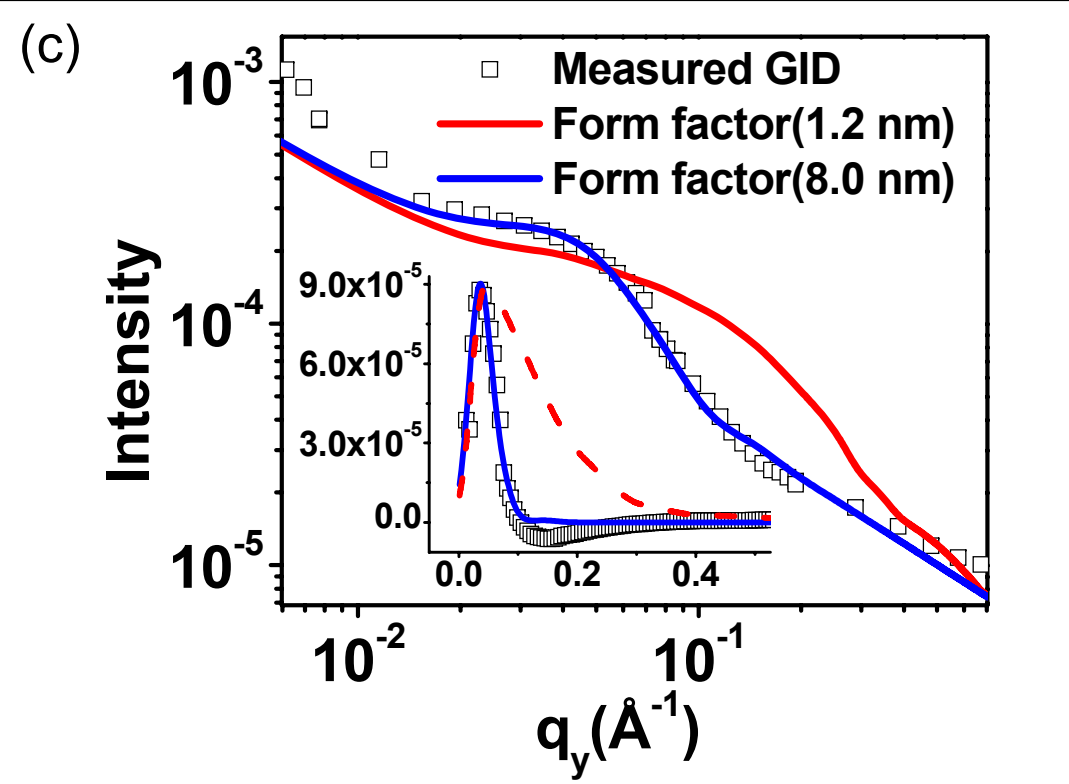
Sanyal, Sinha, Huang
and Ocko,
Phys. Rev. Lett. 66,
628 (1991)

Basu, Hazra and
Sanyal, Phys.
Rev.Lett., 82, 4675
(1999).

$$I(q_y) \propto q_y^{-(2 - \frac{k_B T q_z^2}{2\pi\gamma})}$$

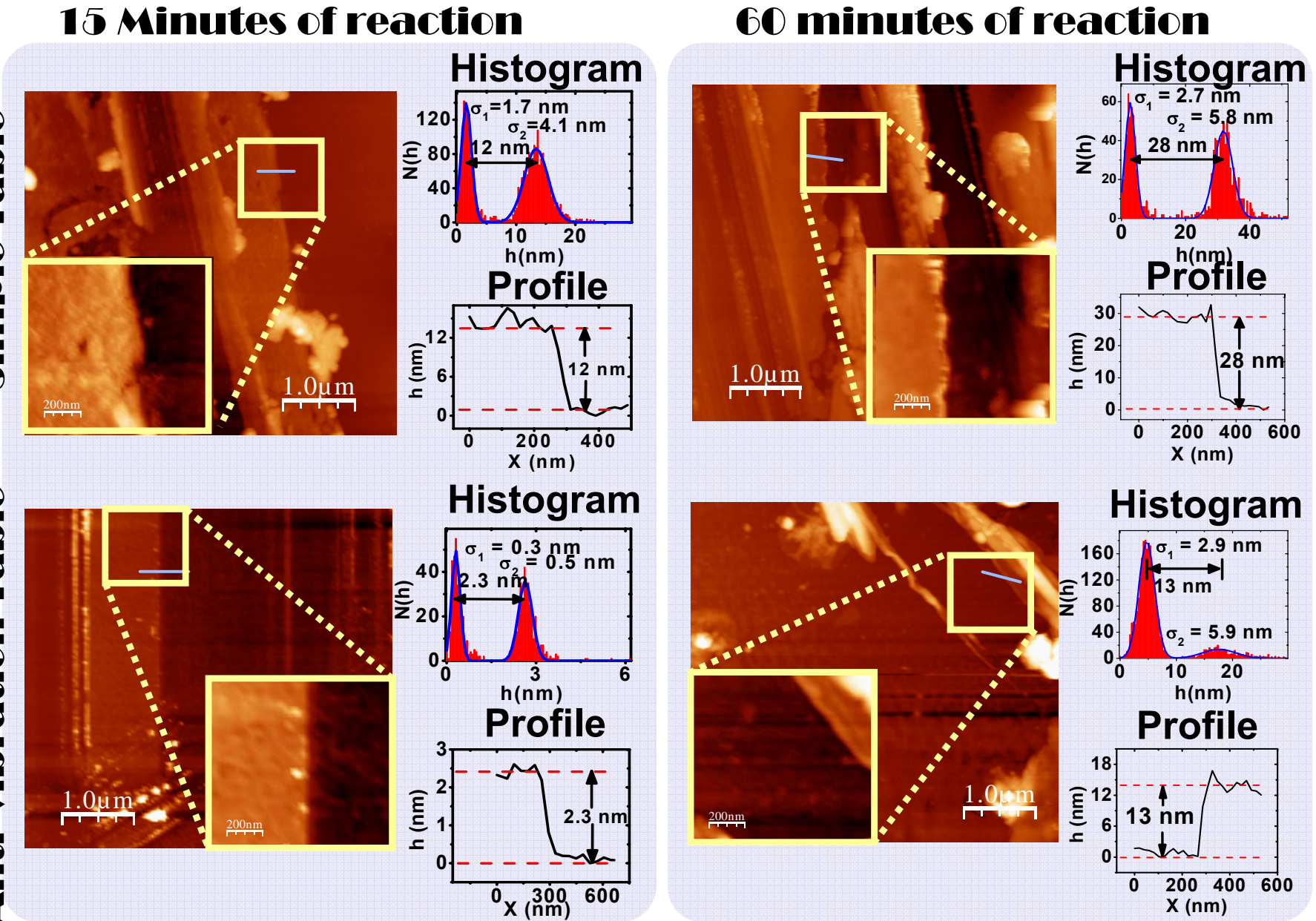
γ : Surface Tension





Effect of External Vibrations

Sample Table Anti-vibration Table

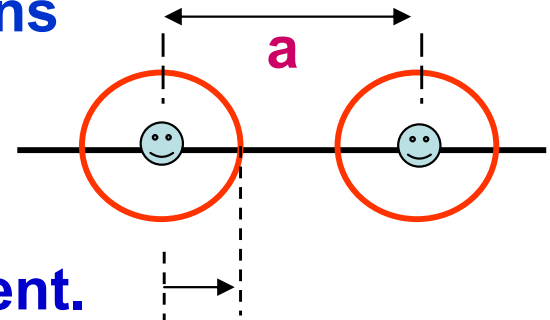


Results obtained so far

- A monolayer of cluster having 13 gold particles of 1.2 nm diameter, similar to that of Au-55 particle, with large (18 nm) in-plane cluster-cluster separation, forms at toluene-water interface. The higher electron density of the top peak indicate presence of Au-55 monolayer.
- Presence of organic layer at interface lowers the surface tension as seen in diffuse measurements. It seems presence of these clusters and associated organic layer hinders the progress of the reaction unless the interface is disturbed by surface pressure and/or vibration.

Wigner Crystallization in Polymer Nanowires

Wigner crystal (WC) → Crystal made of electrons



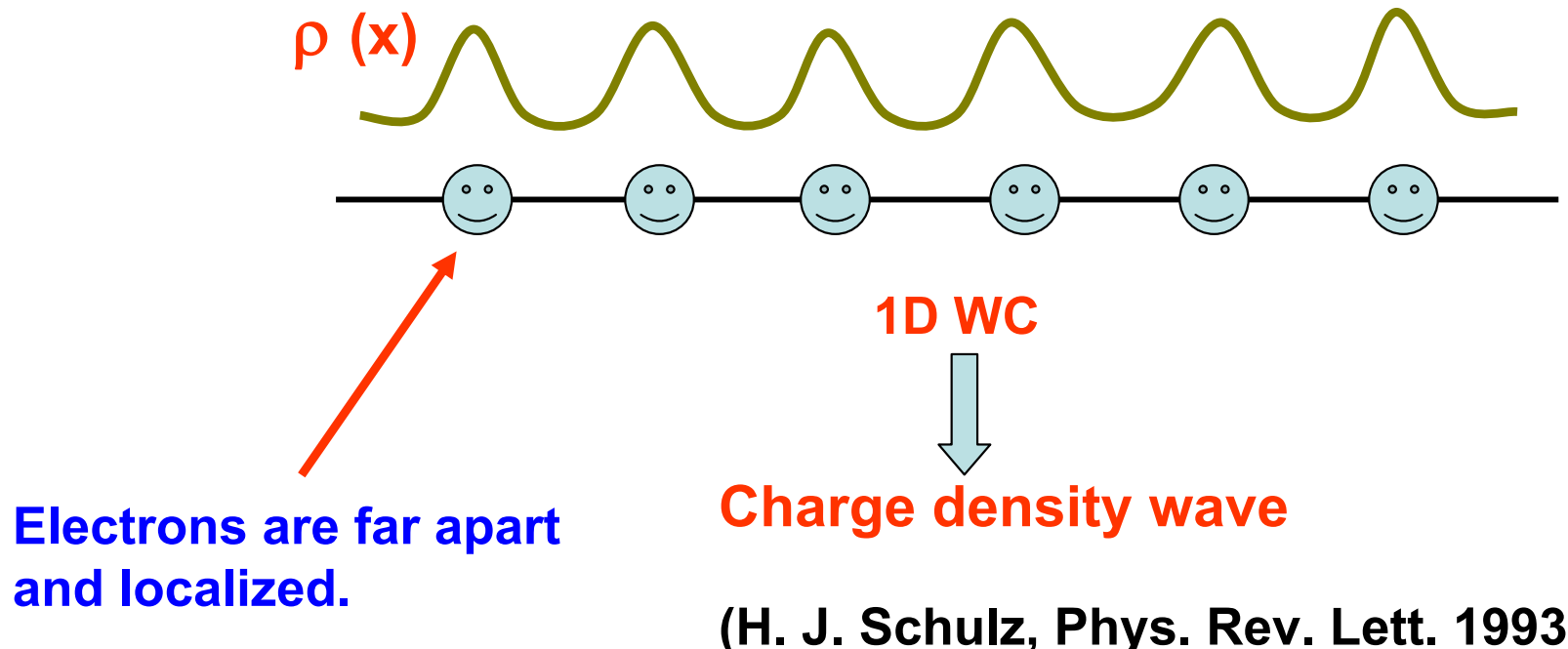
System with low electron density

→ long-range electron-electron interaction is present.

if **Coulombic repulsion > kinetic energy of electrons**

$$r_s (=a/2a_B) \gg 1$$

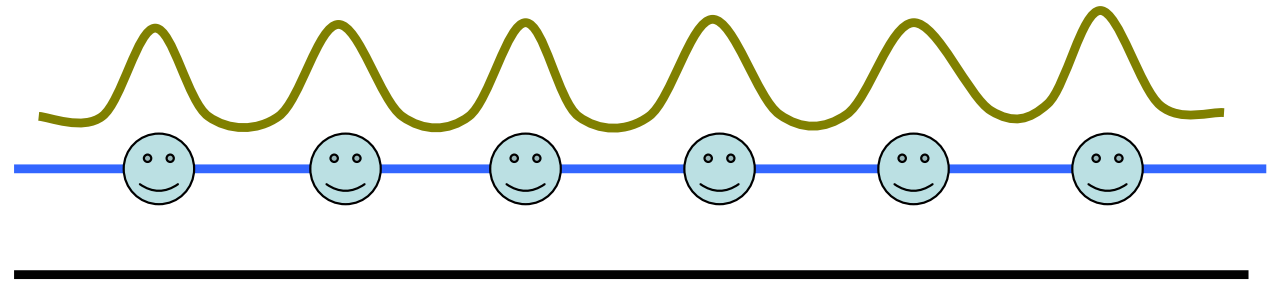
→ electrons get positional ordering ; electron crystal → WC



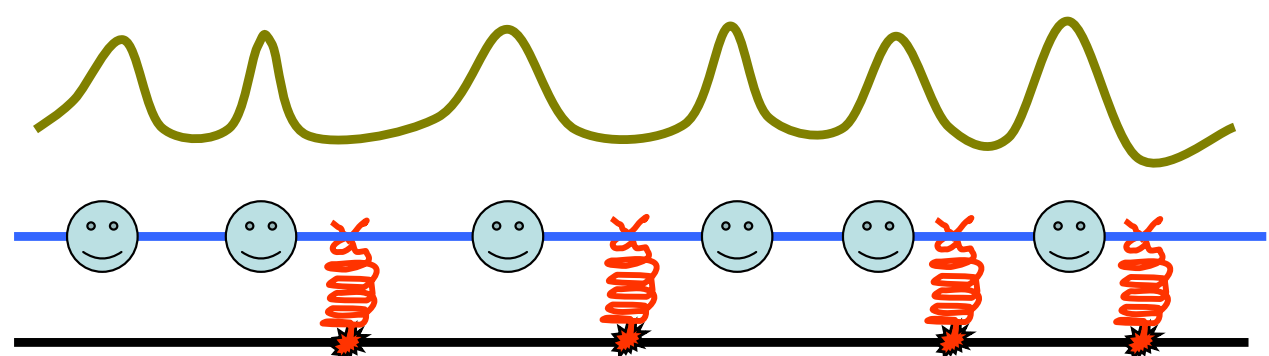
Effect of impurity:

Wigner crystal remains pinned by the impurity

Absence of impurity
Quasi-long-range order



Presence of impurity
Short-range order



Need a threshold voltage (to overcome the pinning barrier) to move the crystal.

Above the threshold bias sliding motion (crystal moves as a whole) starts giving a non-linear I-V characteristics.

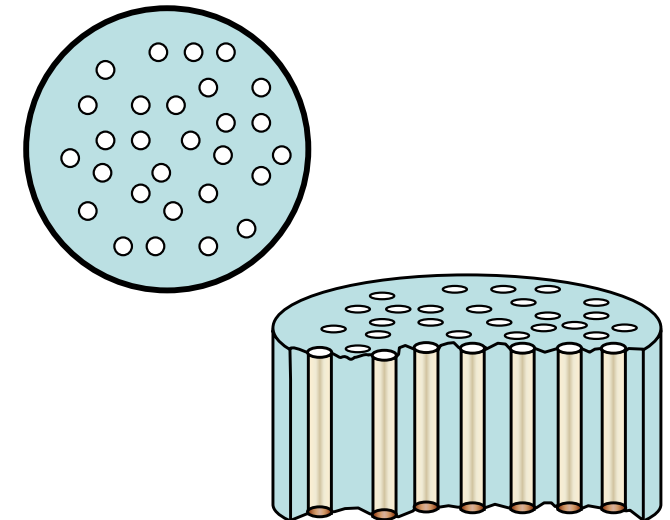
Template based synthesis of Conducting polymer (Polypyrrole) Nanowires

Template → Polycarbonate membrane (pore diameter- 10, 15, 30, 50, 100 and 200 nm)

Reaction → Oxidative polymerization .

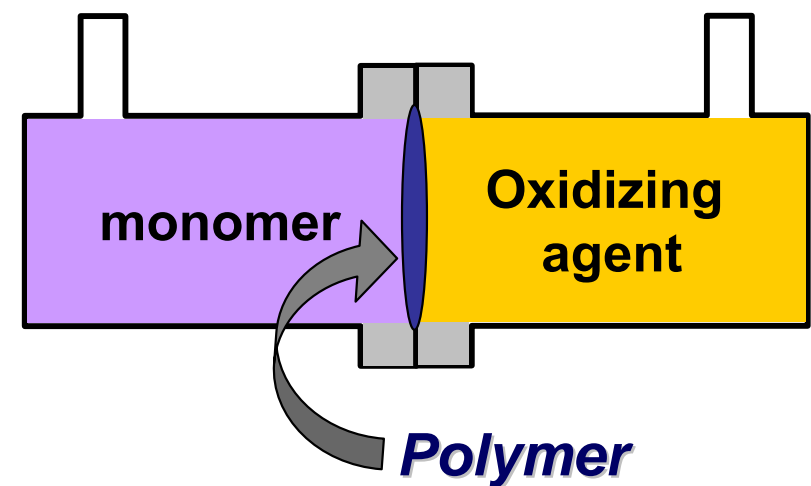
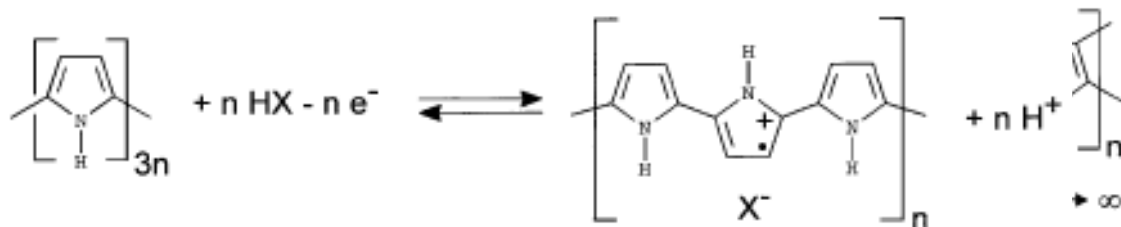
Monomer
Pyrrole

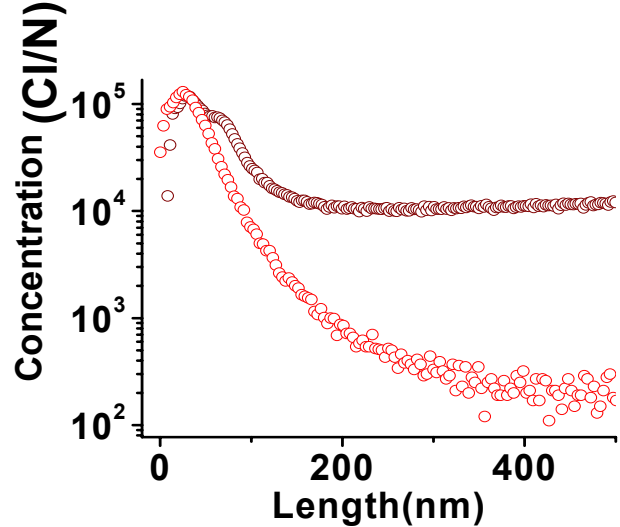
Oxidizing agent
 FeCl_3



Procedure → Membrane placed between two compartment cell.

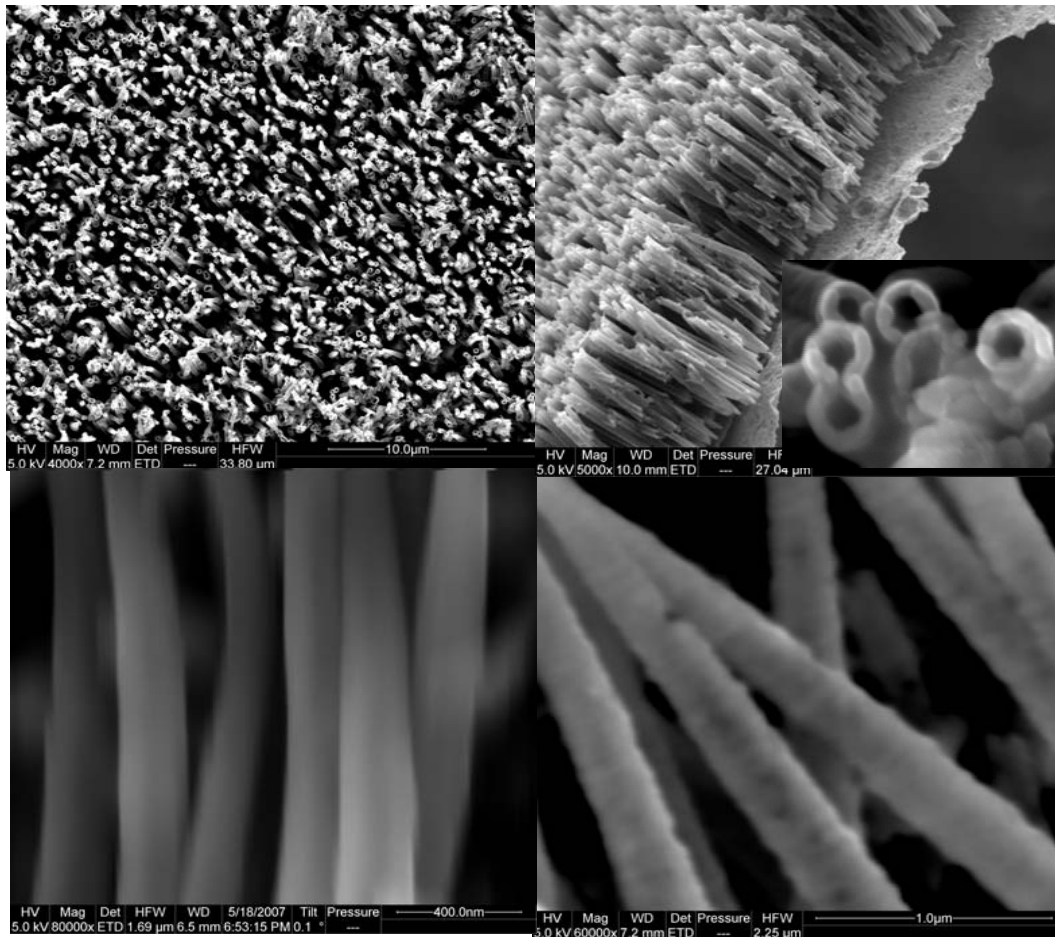
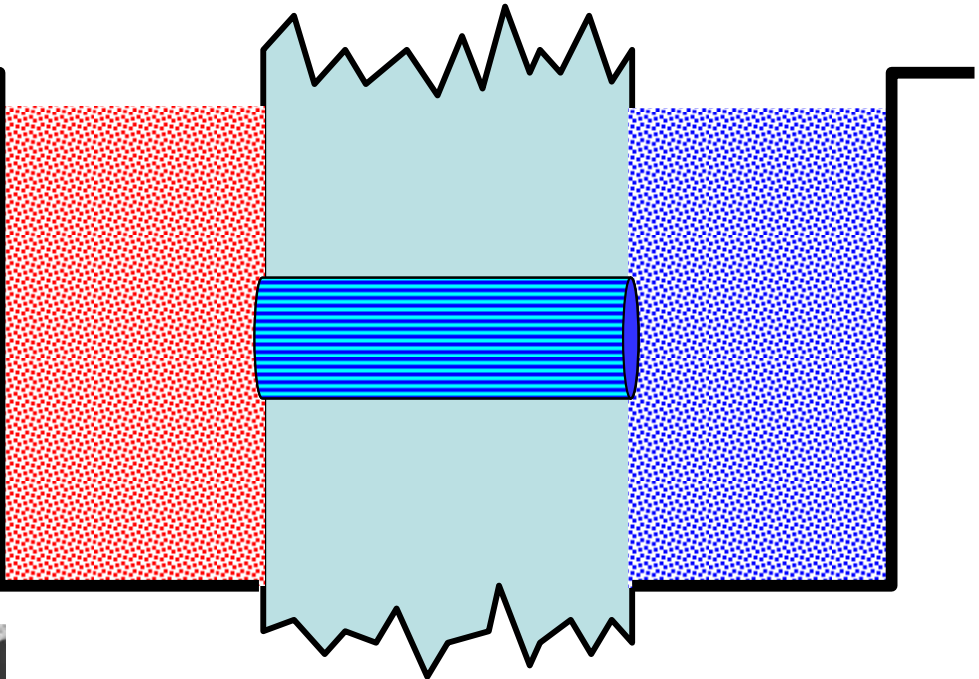
Doping :





200nm

30nm



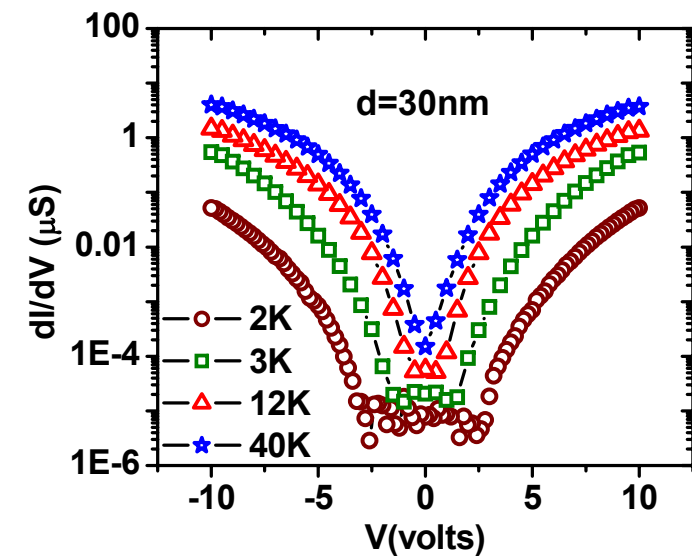
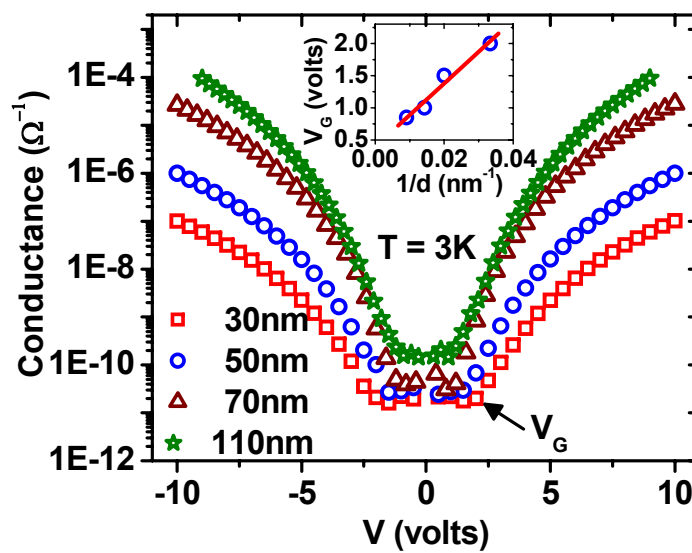
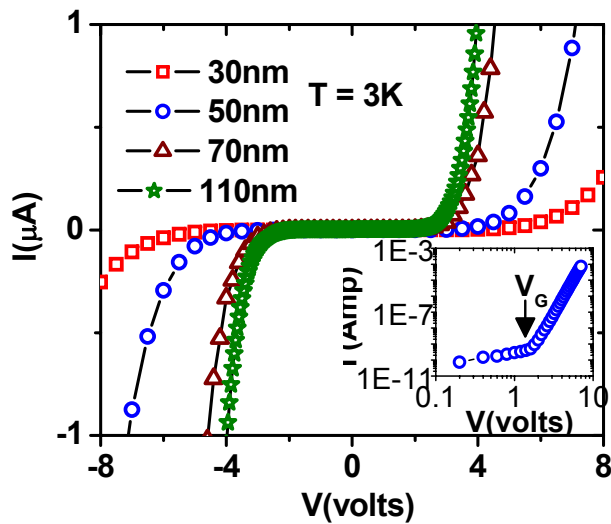
Charge carriers are created by doping (Cl^-) → also acts as impurity.

Chemically synthesized Polymer nanowires have low electron density (electron-electron interaction may play a significant role in determining their electrical property)

Rahman, Sanyal et al.
Phys. Rev. B 73, 125313 (2006)
Chem. Phys. Lett. 447, 268, (2007)

Experimental observations:

I-V and dI/dV -V data of various nanowires shows existence of a 'gap', voltage V_G , above which the conductance increase substantially.



- $V_G \propto d^{-1}$
- V_G vanishes rapidly with increasing T

Gap! Why ?

→ Coulomb blockade (CB)?

Opening of large gap ($\sim 2V$) → can not be explained by CB theory
it would not vanish even at room temperature ($\sim 25\text{meV}$).

→ Collective effect?

In disordered systems the 'gap' opening may occur due to the electron-electron interactions (EEI) between the localized electrons (B. I. Shklovskii and A. L. Efros, *Electronic Properties of Doped Semiconductor*, Springer-Verlag, Berlin, 1984)

Large gap and its temperature dependence suggest electrons are collectively pinned by EEI.

Collective behavior predicted in these nanowires → non-Curie type temperature dependence of static dielectric constant $\epsilon_s \propto T^{-\delta}; \delta > 1$

(A. Rahman et al. *Phys. Rev. B* 73, 125313 (2006)).

Collective behavior may arise due to short range or long range EEI.

Above V_G , I-V characteristics of all nanowires show power law behavior -
 characteristics of 1D conductors.

$$\frac{dI}{dV} \begin{cases} \propto V^\beta & (V \gg k_B T/e) \\ \propto T^\alpha & (V \ll k_B T/e) \end{cases}$$

In 1D conductors

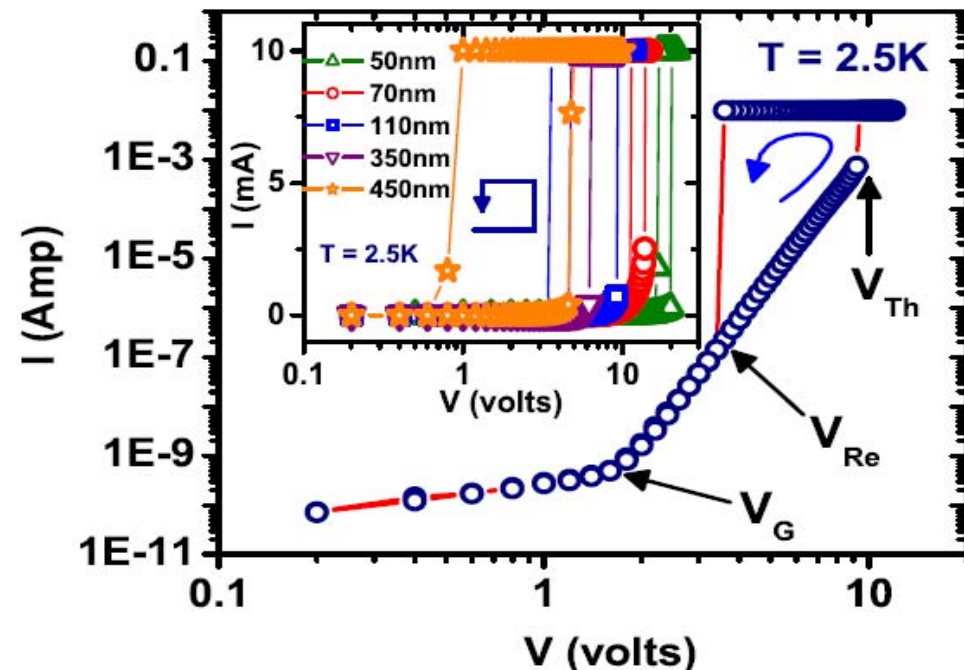
Short range EEI → Luttinger liquid (LL) state.
Long range EEI → Wigner crystal (WC) state.

For LL → I-V curves of different T can be scaled to a master curve by plotting $I/T^{1+\alpha}$ vs. $eV/k_B T$ and $\beta = \alpha$

(L. Balents, cond-mat/9906032)

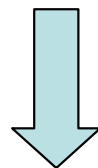
- Existence of gap (V_G),
- Temperature and diameter dependence of V_G
- Power law dependence in I-V characteristics
- Diameter dependence of exponents
- Switching transition (onset of sliding motion)
- Diameter depended switching threshold
- Negative differential resistance
- Noise enhancement in the sliding state

Suggest the formation of pinned Wigner Crystal in these nanowires



Current biased measurements:

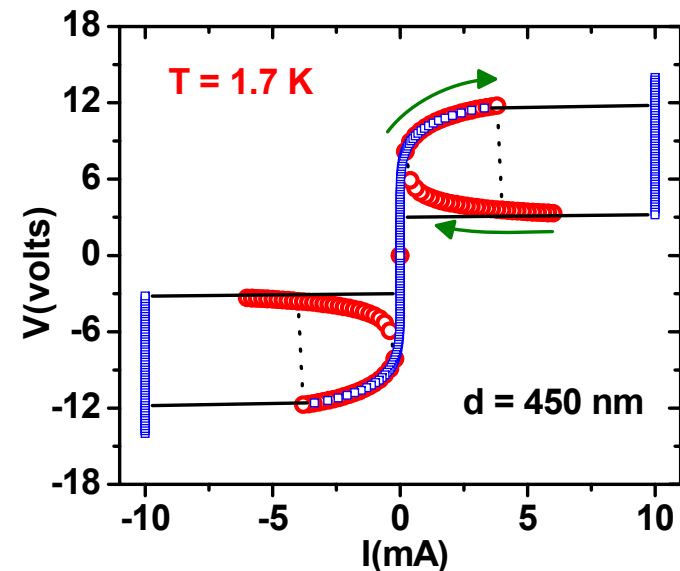
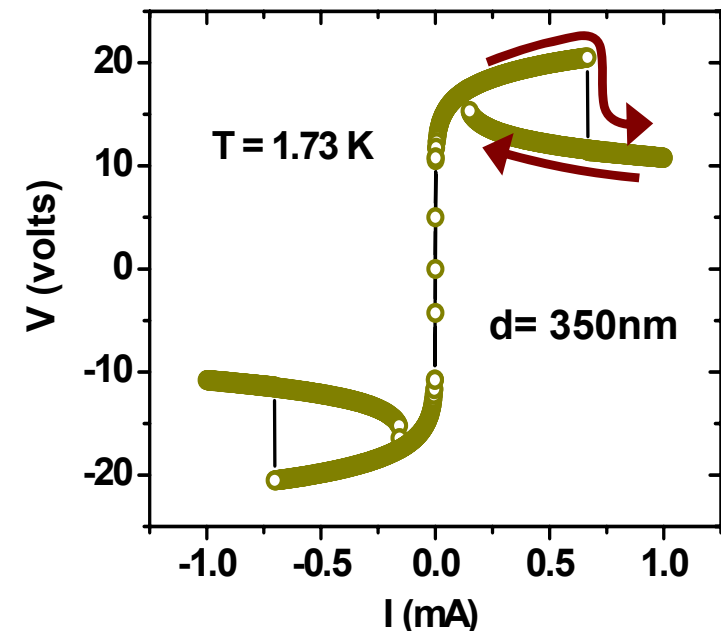
Presence of Negative differential resistance (NDR)



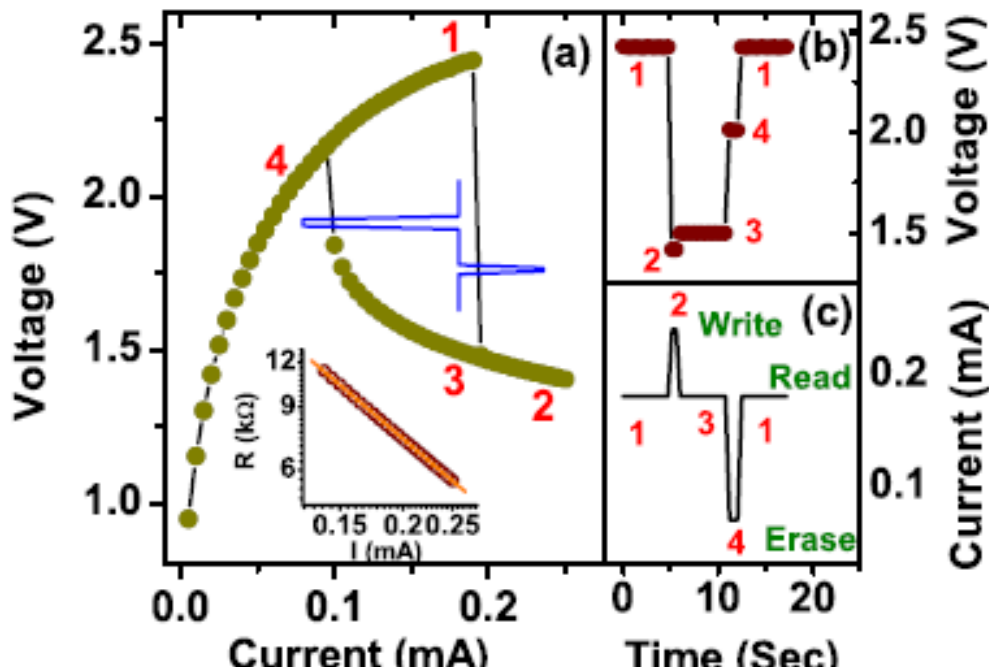
May arises due to opening of large number of parallel channels

Thresholds are **unique** for both current and voltage biased measurement.

Scan speed independence of the results rules out any capacitive effect responsible for NDR.



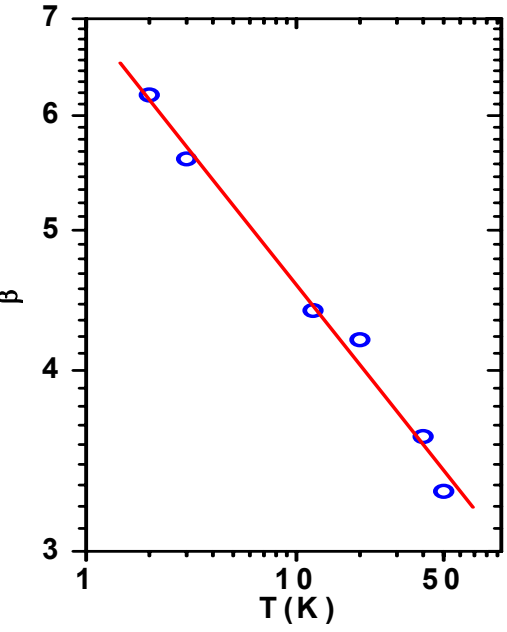
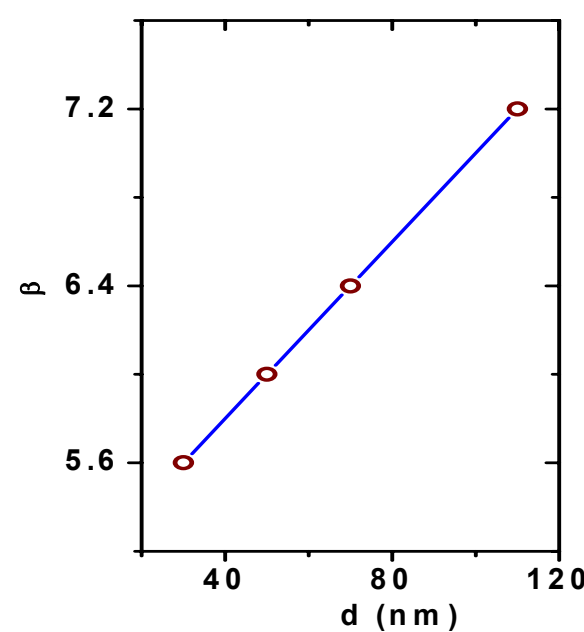
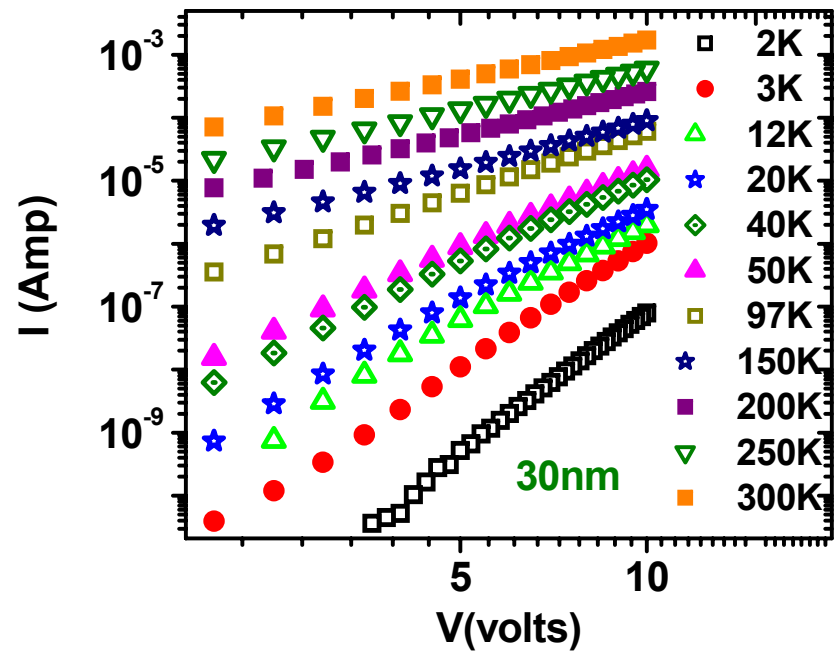
Tunable bistable and multistable memory effect in conducting polymer nanowires



Atikur Rahman and Milan K. Sanyal, *Nanotechnology*. **19**, 395203 (2008).

Highly non-linear current-voltage (I-V) characteristics

I-V characteristics → power law behavior; $I \propto V^{1+\beta}$



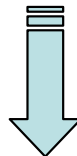
β increases → with increasing diameter (d) of nanowires
with decreasing temperature (T).

$\beta \sim 5 - 7$ at low T . $R \propto T^{-\alpha}$; $\alpha = 1.5 - 5$

$\beta \neq \alpha$

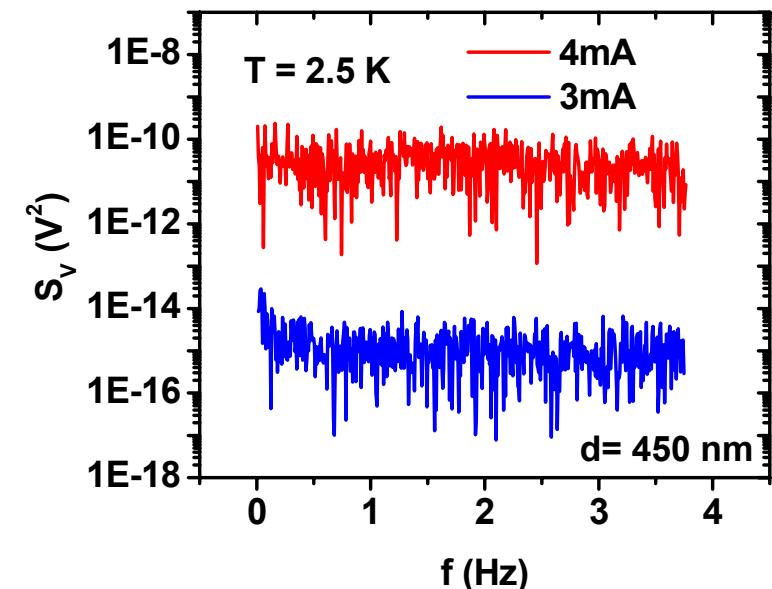
Enhancement of noise in the switched state:

Huge noise enhancement (~ 4 orders of magnitude) was observed in the switched state.



Due to “jerking” motion of strongly correlated electron crystal in the sliding state.

noise decreases rapidly with increasing temperature.



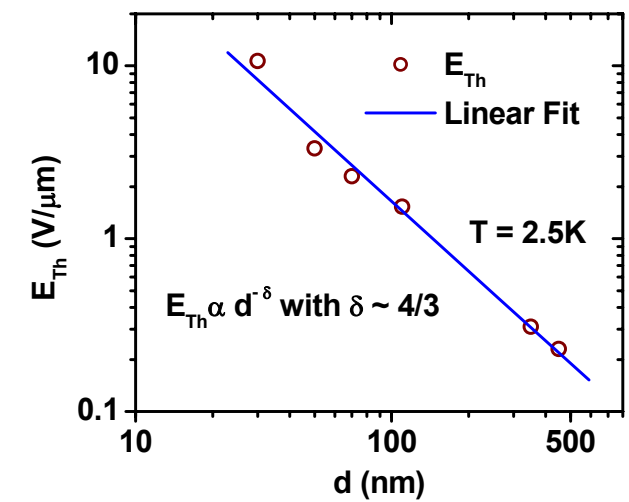
Suggest strongly correlated nature of the system at low T

Nanowires → confined in two directions → 1D pinning

$$E_{\text{Th}} \propto d^{-4/3}$$

(E. Slot et al. Phys. Rev. B, 69 (2004))

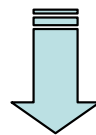
1D WC properties are evident in these nanowires



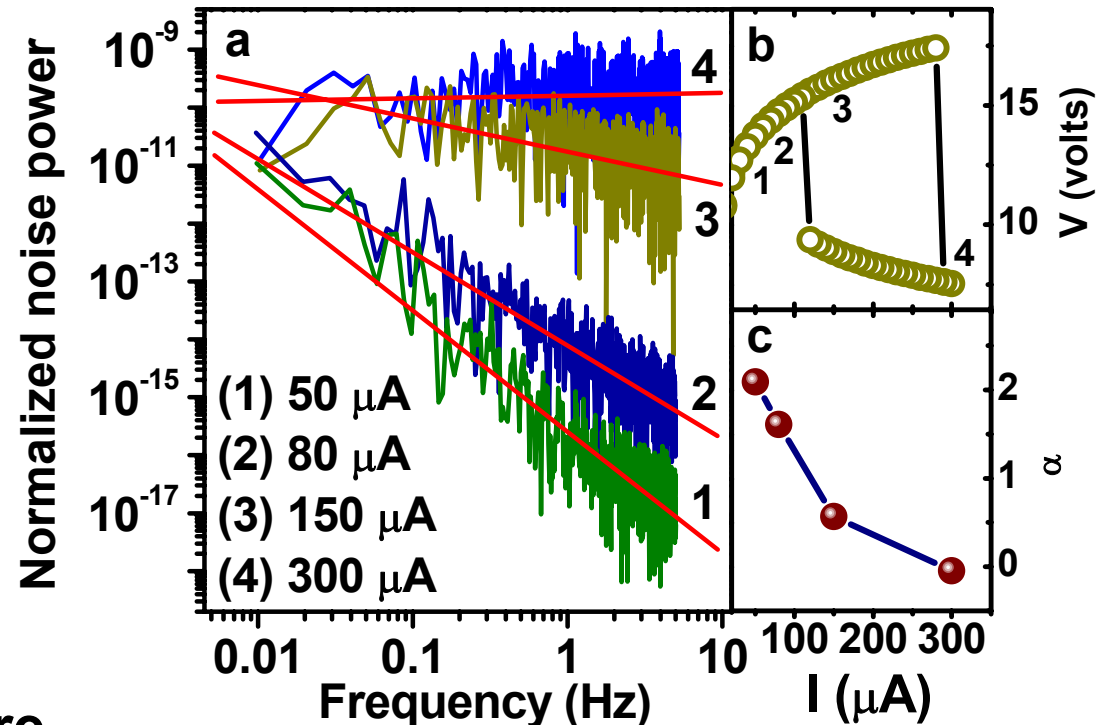
**At low temperature and low bias
Noise power shows a $1/f^\alpha$ type
behavior α can have maximum
value ~ 2 .**

**With increasing bias α decreases
and become independent of
frequency ($\alpha \sim 0$) around the
switching threshold**

**With decreasing bias →
low frequency noise becomes more
dominating → spectral weight
of noise shifts towards lower frequency.**



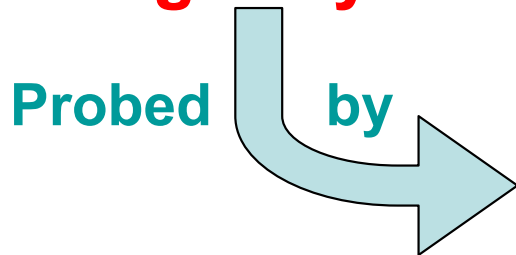
slowing down of electron dynamics



**normalized average noise power increases with increasing bias
→ enhancement of correlation length**

What is about the low bias response

Shows a “**glassy**” behaviour;



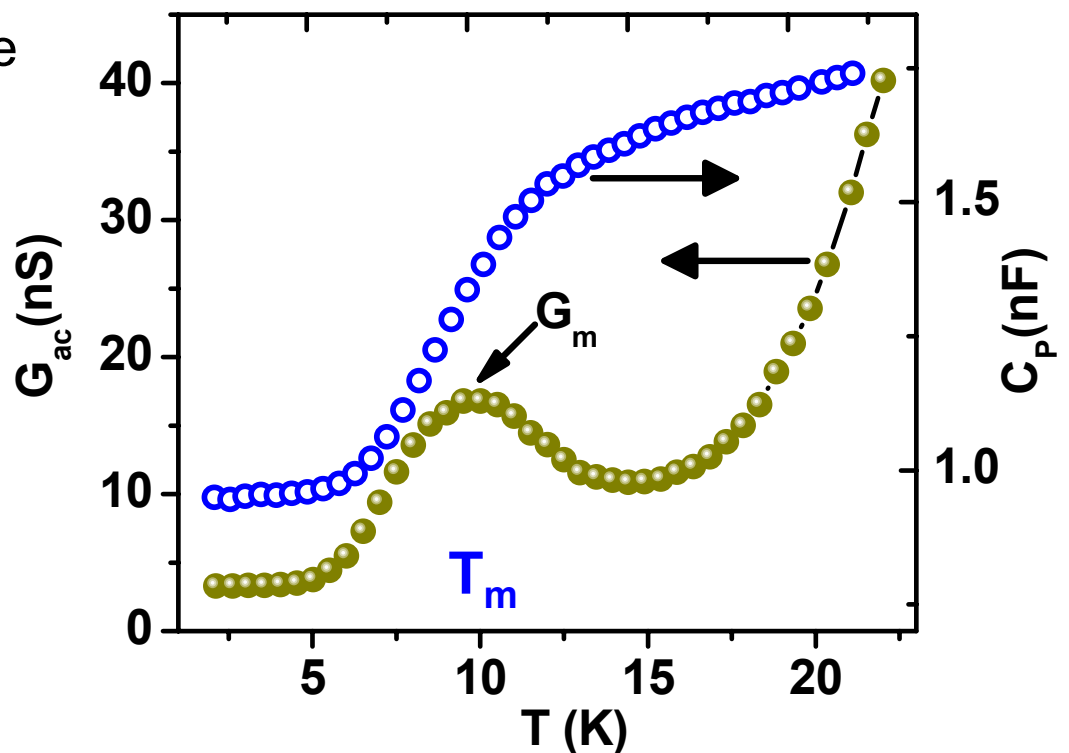
Dielectric relaxation.

Temperature dependence of
ac conductance (G_{ac}) shows a peak
&

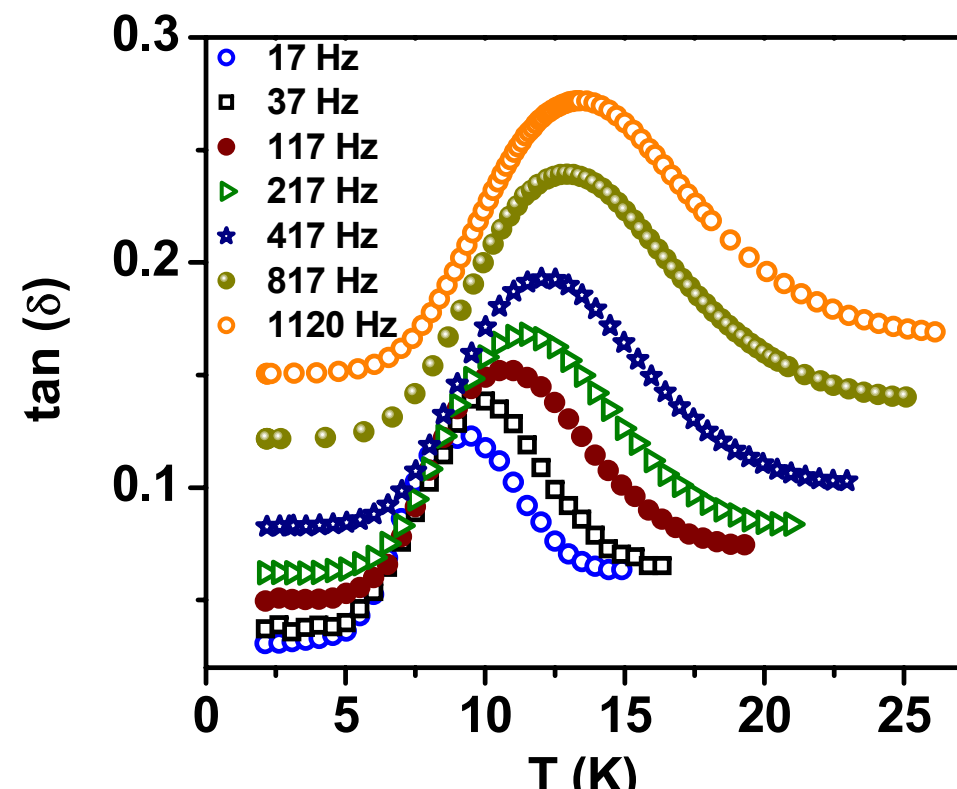
Capacitance (C_p) shows a step like increase

indicates a relaxational behavior

**The temperature (T_m)
corresponding to
conductance peak shifts
with frequency.**



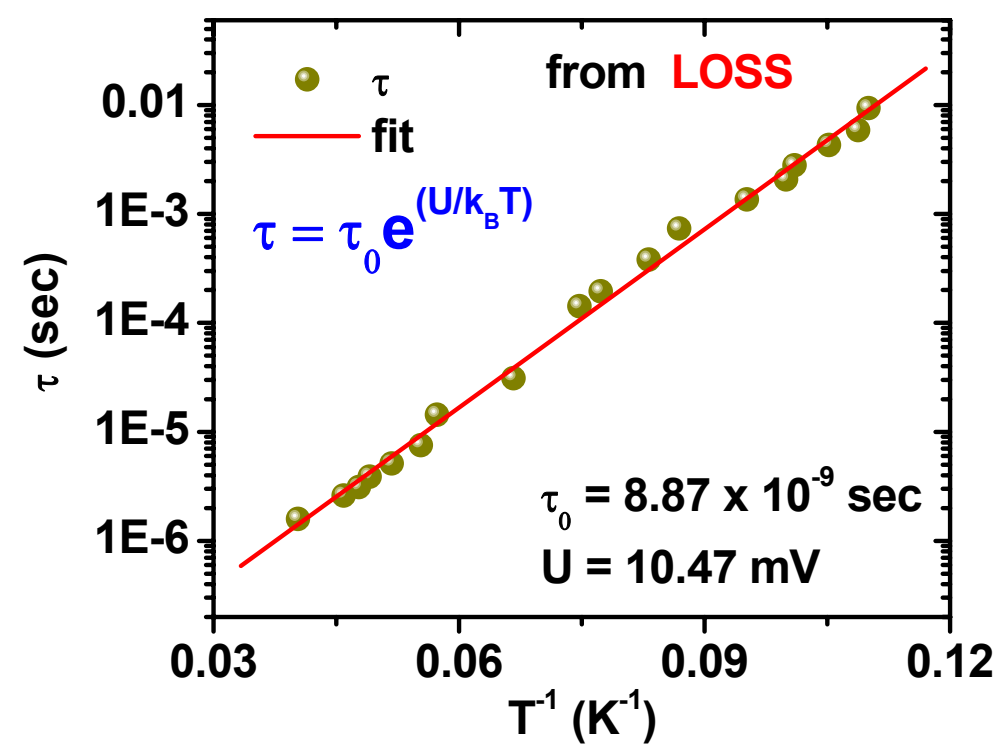
**Peak of “loss tangent”;
 $\tan(\delta) = (\epsilon_2/\epsilon_1)$
shifts to higher temperature
with increasing frequency.**



Mean relaxation time
 $\tau (= 1/(2\pi\nu))$
shows Arrhenius type
temperature dependence

$$\tau = \tau_0 e^{-U/kT}$$

barrier height $U=10.47$ mV



R-T measurements

(with 10 mV dc bias)

when fitted with

$$R = R_0 \exp(\Delta/k_B T)$$

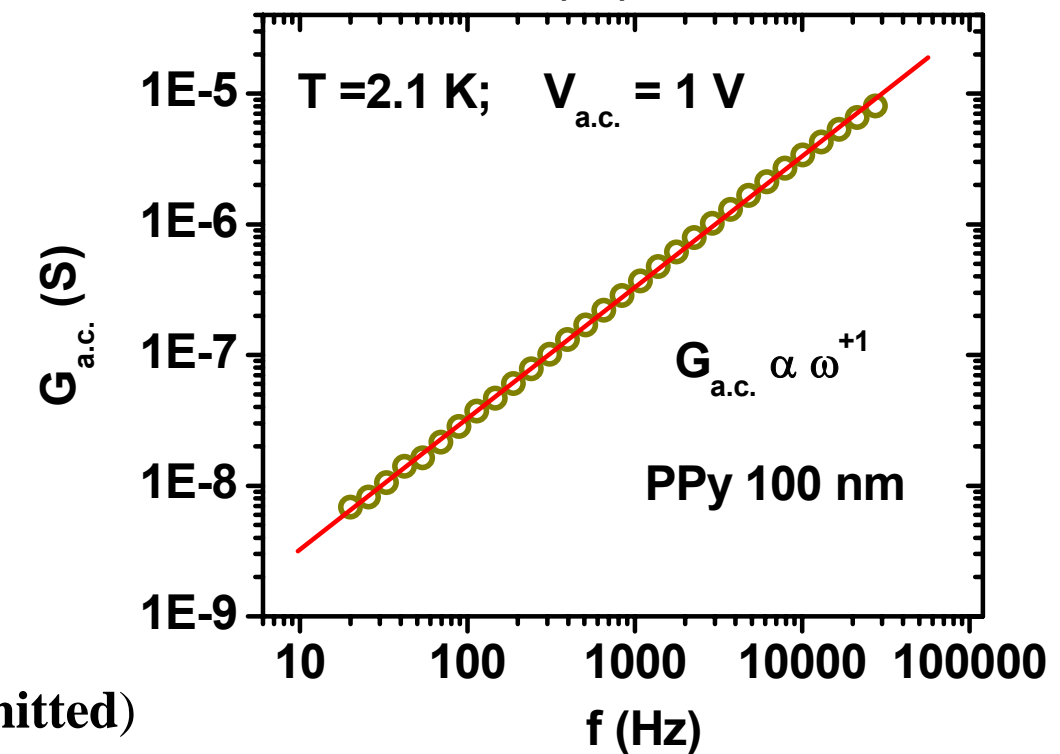
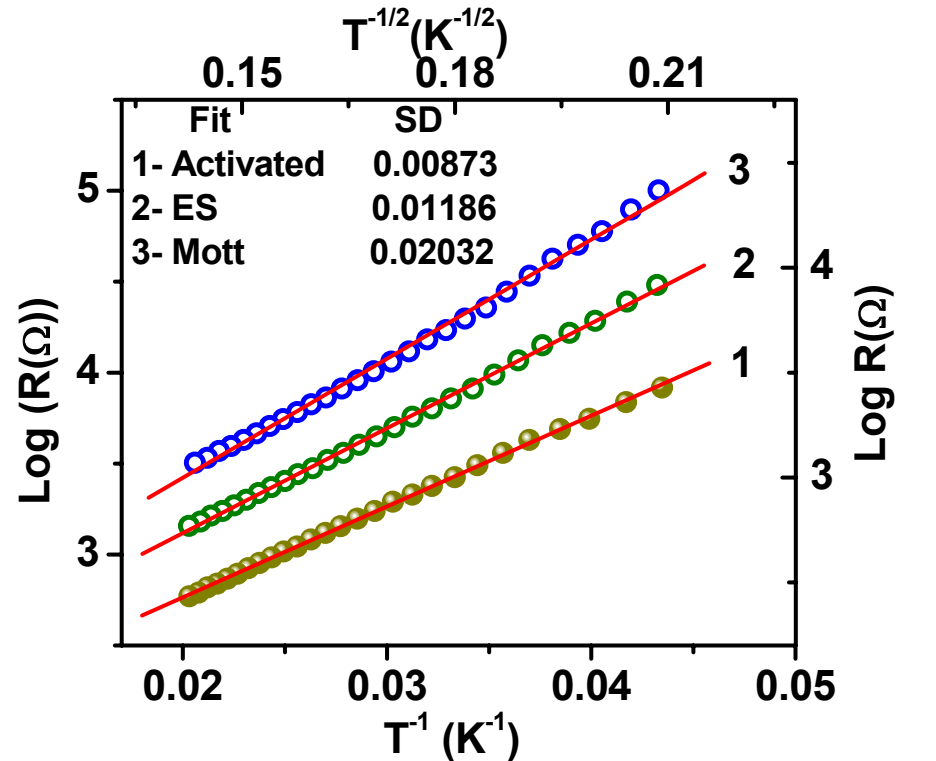
barrier height (Δ) ~ 9.6 meV

Conductance shows linear Dependence on frequency

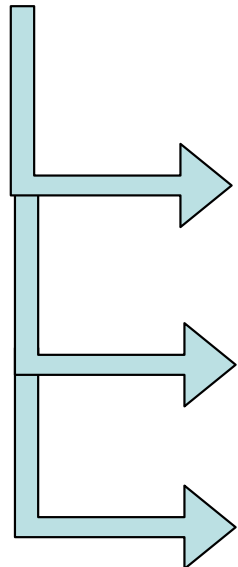
$$G_{\text{a.c.}} \propto \omega$$

Characteristics of
Wigner/Coulomb glass

Atikur Rahman and Milan K. Sanyal, (Submitted)



Anderson localized electrons



no e-e interaction \rightarrow Fermi glass [$G_{a.c.} \propto \omega^2$]

e-e interaction (weak) \rightarrow Coulomb glass [$G_{a.c.} \propto \omega$]

e-e interaction (strong) \rightarrow Wigner glass [$G_{a.c.} \propto \omega$]

Difference ?

Coulomb glass

&

Wigner glass

Theory

No ordering
of electrons

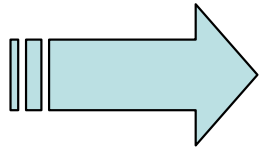
Power-law ordering
of electrons

Experiment

?

S. Charkravarty et. al. *Philos. Mag. B* 79, 859 (1999)

**With increasing bias the pinning becomes less effective
→ correlation length increases**



**Small ordering of electrons
may exist at low temperature
and low bias →
Wigner Glass !**

Increasing bias

Wigner Glass



Wigner Crystal

Our main results

- All the nanowires have three distinct regions: Below V_G current is very small and that increases with temperature and diameter. Between V_G and V_{Th} power-law characteristics of 1D transport is observed. Above V_{Th} switching transition is observed that exhibit hysteresis, $d^{-4/3}$ scaling, NDR and 'noise' enhancement.
- Observation of negative differential resistance and noise enhancement in the sliding state reconfirms the presence of charge density wave (CDW) as expected in 1DWC [theoretically predicted by Fogler et al Phys. Rev. B69, 035413 (2004) for disordered lattice]
- Exhibit “Glassy Behavior” at low bias –expected for electrons localized in random potential and not free to move.
(Slutskin, Pepper and Kovtun, Europhys. Lett. 62, 705, 2003)

Thank You